

# A RESTRICTED SVD TYPE CUR DECOMPOSITION FOR MATRIX TRIPLET<sup>\*</sup>

PERFECT Y. GIDISU<sup>†</sup> AND MICHIEL E. HOCHSTENBACH<sup>†</sup>

**Abstract.** We propose a restricted SVD based CUR (RSVD-CUR) decomposition for matrix triplets  $(A, B, G)$ . Given matrices  $A$ ,  $B$ , and  $G$  of compatible dimensions, such a decomposition provides a coupled low-rank approximation of the three matrices using a subset of their rows and columns. We pick the subset of rows and columns of the original matrices by applying the discrete empirical interpolation method (DEIM) to the orthogonal and nonsingular matrices from the restricted singular value decomposition of the matrix triplet. We investigate the connections between this DEIM type RSVD-CUR approximation and a DEIM type CUR factorization, and a DEIM type generalized CUR decomposition. We provide an error analysis that shows that the accuracy of the proposed RSVD-CUR decomposition is within a factor of the approximation error of the restricted singular value decomposition of given matrices. An RSVD-CUR factorization may be suitable for applications where we are interested in approximating one data matrix relative to two other given matrices. Two applications that we discuss include multi-view and multi-label dimension reduction, and data perturbation problems of the form  $A_E = A + BFG$ , where  $BFG$  is a correlated noise matrix. In numerical experiments, we show the advantages of the new method over the standard CUR approximation for these applications.

**Key words.** Restricted SVD, low-rank approximation, CUR decomposition, interpolative decomposition, DEIM, subset selection, canonical correlation analysis, multi-view learning, nonwhite noise, colored noise, structured perturbation

**MSC codes.** 65F55, 15A23, 15A18, 15A21, 65F15, 68W25

**1. Introduction.** Identifying the underlying structure of a data matrix and extracting meaningful information is a crucial problem in data analysis. Low-rank matrix approximation is one of the means to achieve this. CUR factorizations and interpolative decompositions (ID) are appealing techniques for low-rank matrix approximations, which approximate a data matrix in terms of a subset of its columns and rows. These types of low-rank matrix factorizations have several advantages over the ones based on orthonormal bases because they inherit properties such as sparsity, nonnegativity, and interpretability of the original matrix. Various proposed algorithms in the literature seek to find a representative subset of rows and columns by exploiting the properties of the singular vectors [22, 25] or using a pivoted QR factorization [29]. Given a matrix  $A \in \mathbb{R}^{m \times n}$  and a target rank  $k$ , a rank- $k$  CUR factorization approximates  $A$  as

$$(1.1) \quad \begin{array}{c} A \\ m \times n \end{array} \approx \begin{array}{c} C \\ m \times k \end{array} \begin{array}{c} M \\ k \times k \end{array} \begin{array}{c} R \\ k \times n \end{array},$$

where  $C$  and  $R$  (both of rank  $k$ ) consist of  $k$  columns and rows of  $A$ , respectively. The middle matrix  $M$  (of rank  $k$ ) can be computed as  $(C^T C)^{-1} C^T A R^T (R R^T)^{-1}$ ; in [26], Stewart shows how this computation minimizes  $\|A - CMR\|$  for specified row and column indices. Here,  $\|\cdot\|$  denotes the spectral norm. To construct the factors  $C$  and  $R$ , one can apply the discrete empirical interpolation method (DEIM) proposed in [4] or any other appropriate index selection method (see, e.g., [16, 22, 9]) to the leading  $k$  right and left singular vectors of  $A$ .

<sup>\*</sup>Version November 15, 2022.

**Funding:** This work has received funding from the European Union's Horizon 2020 research and innovation programme under the Marie Skłodowska-Curie grant agreement No 812912.

<sup>†</sup>Department of Mathematics and Computer Science, TU Eindhoven, The Netherlands, (p.gidisu@tue.nl, m.e.hochstenbach@tue.nl).

In this paper, we generalize the DEIM type CUR [25] method to develop a new coupled CUR factorization of a matrix triplet  $(A, B, G)$  of compatible dimensions, based on the restricted singular value decomposition (RSVD). We call this factorization an RSVD based CUR (RSVD-CUR) factorization. We stress that this RSVD does not stand for randomized SVD (see, e.g., [17]).

Over the decades, several generalizations of the singular value decomposition (SVD) corresponding to the product or quotient of two to three matrices have been proposed. The most commonly known generalization is the generalized SVD (GSVD), also referred to as the quotient SVD of a matrix pair  $(A, B)$  [6], which corresponds to the SVD of  $AB^{-1}$  if  $B$  is square and nonsingular. Another generalization is the RSVD of a matrix triplet  $(A, B, G)$  [32] which shows the SVD of  $B^{-1}AG^{-1}$  if  $B$  and  $G$  are square and nonsingular. Similarly, we have proposed generalizations of an SVD-based CUR decomposition: first, a generalized CUR (GCUR) decomposition of a matrix pair  $(A, B)$  in [12]; second, in this paper, an RSVD-CUR decomposition of a matrix triplet  $(A, B, G)$ . We emphasize that an RSVD-CUR is more general than a GCUR decomposition. One can derive a GCUR decomposition from an RSVD-CUR factorization given special choices of the matrices  $B$  or  $G$  (we will see this in [Proposition 4.2](#)); however, we note that the converse does not hold. Both CUR decomposition and RSVD algorithms have been well-studied. However, to the best of our knowledge, this work is the first to combine both methods. The RSVD has been around for over three decades now; this new method introduces a new type of exploitation of the RSVD.

In recent times, many real-world data sets often comprise different representations or views, which provide information complementary to each other. Our RSVD-CUR factorization is motivated by the canonical correlation analysis (CCA) of a matrix pair  $(B, G)$  (see, e.g., [14]), which is related to the RSVD of the matrix triplet  $(G^TB, G^T, B)$  (see [sections 2](#) and [3](#)). CCA is one of the most common techniques for multi-data processing [19, pp. 443–454]. CCA aims to find a pair of linear transformations, one for each set of features, such that when the sets of variables are transformed, the corresponding coordinates are maximally correlated [19, p. 443]. Here, we aim to find subsets of columns or rows of  $B$  and  $G$  by exploiting some of the basis vectors of  $B$  and  $G$  that maximize the pairwise correlations across the two matrices. We expect that an RSVD-CUR factorization may be useful for multi-view dimension reduction and integration of information from multiple views in multi-view learning. Multi-view learning is a rapidly growing direction in machine learning that involves learning with multiple views to improve the generalization performance (see, e.g., [31]). Analogous to CCA, an RSVD-CUR factorization as a tool for multi-view dimension reduction can cope with a two-view case. In the same context, we also expect that one could use an RSVD-CUR as a supervised feature selection technique in multilabel classification problems (see [section 5](#)). In this setting, one view is obtained from the data and another from the class labels.

Another motivation for an RSVD-CUR factorization stems from applications where the goal is to select a subset of rows and columns of one data set relative to two other data sets. An example is a data perturbation problem of the form  $A_E = A + BFG$  where  $BFG$  is a correlated noise matrix (see, e.g., [3, 32]) and the goal is to recover the low-rank matrix  $A$  from  $A_E$  given the structure of  $B$  and  $G$ . Conventionally, when faced with this kind of perturbation problem, to use an SVD-based method, a prewhitening step is required to make the additive noise a white noise. However, with the RSVD formulation, the prewhitening operation becomes an integral part of the algorithm. It is worth pointing out that one does not neces-

sarily need to know the exact noise covariance matrices; the RSVD and RSVD-CUR may still deliver good approximation results given inexact covariance matrices (see [section 5](#)). An example of an inexact covariance matrix is when we approximate the population covariance matrix by a sample covariance matrix.

Considering the ordinary or total least squares problem of the form  $A\mathbf{x} \approx b$ , in many applications, it is desirable to reduce the number of variables that are to be considered or measured in the future. For instance, the modeler may not be interested in a predictor such as  $A\mathbf{x}$  with all redundant variables but rather  $A\hat{\mathbf{x}}$ , where  $\hat{\mathbf{x}}$  has at most  $k$  nonzero entries. The position of the nonzero entries determines which columns of  $A$ , i.e., which variables to use in the model for approximating the response vector  $\mathbf{b}$ . How to pick these columns is the problem of subset selection, and one can use a CUR factorization algorithm. Consider the setting of generalized Gauss-Markov models with constraints, i.e.,

$$(1.2) \quad \min_{\mathbf{x}, \mathbf{y}, \mathbf{f}} \|\mathbf{y}\|^2 + \|\mathbf{f}\|^2 \quad \text{subject to} \quad \mathbf{b} = A\mathbf{x} + B\mathbf{y}, \quad \mathbf{f} = G\mathbf{x},$$

where  $A, B, G, \mathbf{b}$  are given. Notice that where  $B = I$  and  $G = 0$ , this formulation is a generalization of the traditional least squares problem. Since this equation involves three matrices, an appropriate tool for its analysis will be the RSVD [[8](#), [18](#)]. For variable subset selection in this problem, the RSVD-CUR may be a suitable method that incorporates the error and the constraints.

**Outline.** A short review of CCA is provided in [section 2](#). [Section 3](#) gives a brief overview of the RSVD. [Section 4](#) introduces the new RSVD-CUR decomposition. In this section, we also discuss some error bounds. [Algorithm 4.3](#) summarizes the procedure of constructing a DEIM type RSVD-CUR decomposition. Results of numerical experiments using synthetic and real data sets are presented in [section 5](#), followed by conclusions in [section 6](#).

**2. Canonical Correlation Analysis.** This section briefly discusses CCA, one of our motivations for the proposed RSVD-CUR approximation. CCA is one of the most widely used and valuable techniques for multi-data processing. It is used to analyze the mutual relationships between two sets of variables and finds a wide range of applications across many different fields. In a web classification problem, usually, a web document can be described by either the words occurring on the page (this, for instance, can be matrix  $B$ ) or the words contained in the anchor text of links pointing to this page (and can be taken as matrix  $G$ ). In a genome-wide association study, CCA is used to discover the genetic associations between genotype data of single nucleotide polymorphisms (SNPs) contained in  $B$  and phenotype data of gene expression levels contained in  $G$  [[5](#)]. In information retrieval, CCA is used to embed both the search space (e.g., images) and the query space (e.g., text) into a shared low dimensional latent space so that the closeness between the queries and the candidates can be quantified [[23](#)]. Other applications include fMRI data analysis [[11](#)], natural language processing, and speech recognition [[1](#)].

Let  $B \in \mathbb{R}^{m \times \ell}$ ,  $G \in \mathbb{R}^{d \times n}$  with  $m = d$ , be of full column rank and  $k \leq \min(\ell, n)$ . CCA seeks to find the linear combinations of the form  $B\mathbf{w}_i$  and  $G\mathbf{z}_i$  for  $i = 1, \dots, k$  that maximize the pairwise correlations across the two matrices [[19](#), p. 443]. We can define the canonical correlations  $\rho_1(B, G), \dots, \rho_k(B, G)$  of the matrix pair  $(B, G)$  as

[14]

$$(2.1) \quad \rho_i(B, G) = \max_{\substack{B\mathbf{w} \neq \mathbf{0}, G\mathbf{z} \neq \mathbf{0} \\ B\mathbf{w} \perp \{B\mathbf{w}_1, \dots, B\mathbf{w}_{i-1}\} \\ G\mathbf{z} \perp \{G\mathbf{z}_1, \dots, G\mathbf{z}_{i-1}\}}} \rho(G\mathbf{z}, B\mathbf{w}) =: \rho(G\mathbf{z}_i, B\mathbf{w}_i) := \frac{\mathbf{z}_i^T G^T B \mathbf{w}_i}{\|G\mathbf{z}_i\| \|B\mathbf{w}_i\|}.$$

We have that  $\rho_1(B, G) \geq \dots \geq \rho_k(B, G)$ . The vectors of unit length  $G\mathbf{z}_i/\|G\mathbf{z}_i\|$  and  $B\mathbf{w}_i/\|B\mathbf{w}_i\|$  are referred to as the canonical vectors of  $(B, G)$  and the canonical weights are  $\mathbf{z}_i/\|G\mathbf{z}_i\|$  and  $\mathbf{w}_i/\|B\mathbf{w}_i\|$ . As discussed in [14], there are several equivalent ways to formulate CCA. We show a Lagrange multiplier formulation which is suitable for our context and will serve as a motivation for the proposed decomposition. The Lagrange multiplier function of the above constrained optimization problem is [14]

$$f(\mathbf{w}, \mathbf{z}, \lambda, \mu) = \mathbf{z}^T G^T B \mathbf{w} - \frac{1}{2} \lambda (\|B\mathbf{w}\|^2 - 1) - \frac{1}{2} \mu (\|G\mathbf{z}\|^2 - 1).$$

We note that  $\rho_i(B, G)$  is not affected by the rescaling of  $B\mathbf{w}_i$  and  $G\mathbf{z}_i$ . We, therefore, maximize the problem subject to the constraints  $\mathbf{w}^T B^T B \mathbf{w} = 1$  and  $\mathbf{z}^T G^T G \mathbf{z} = 1$ . Differentiating the above with respect to  $\mathbf{z}$  and  $\mathbf{w}$  gives

$$\begin{aligned} G^T B \mathbf{w} - \mu G^T G \mathbf{z} &= \mathbf{0}, \\ B^T G \mathbf{z} - \lambda B^T B \mathbf{w} &= \mathbf{0}. \end{aligned}$$

Premultiplying the above equations by  $\mathbf{z}^T$  and  $\mathbf{w}^T$ , respectively, together with the constraints  $\mathbf{w}^T B^T B \mathbf{w} = 1$  and  $\mathbf{z}^T G^T G \mathbf{z} = 1$ , we have that  $\lambda = \mu$  and

$$(2.2) \quad \begin{bmatrix} & G^T B \\ B^T G & \end{bmatrix} \begin{bmatrix} \mathbf{z} \\ \mathbf{w} \end{bmatrix} = \lambda \begin{bmatrix} G^T G & \\ & B^T B \end{bmatrix} \begin{bmatrix} \mathbf{z} \\ \mathbf{w} \end{bmatrix}.$$

The canonical weights and correlations are the generalized eigenvectors and eigenvalues, respectively, of this generalized eigenvalue problem. We will show in the next section how this problem relates to the RSVD of matrix triplets which we exploit for our proposed RSVD-CUR factorization.

**3. Restricted SVD.** The RSVD of matrix triplets, as notably studied in [32, 8], is an essential building block for the proposed decomposition in this paper. We give a brief overview of this matrix factorization here. The RSVD may be viewed as a decomposition of a matrix relative to two other matrices of compatible dimensions. Given a matrix triplet  $A \in \mathbb{R}^{m \times n}$ ,  $B \in \mathbb{R}^{m \times \ell}$ , and  $G \in \mathbb{R}^{d \times n}$ , following the formulation in [32], there exist orthogonal matrices  $U \in \mathbb{R}^{\ell \times \ell}$  and  $V \in \mathbb{R}^{d \times d}$ , and nonsingular matrices  $Z \in \mathbb{R}^{m \times m}$  and  $W \in \mathbb{R}^{n \times n}$  such that

$$(3.1) \quad A = Z D_A W^T, \quad B = Z D_B U^T, \quad G = V D_G W^T,$$

which implies

$$\begin{bmatrix} A & B \\ G & \end{bmatrix} = \begin{bmatrix} Z & \\ & V \end{bmatrix} \begin{bmatrix} D_A & D_B \\ D_G & \end{bmatrix} \begin{bmatrix} W & \\ & U \end{bmatrix}^T.$$

where  $D_A \in \mathbb{R}^{m \times n}$ ,  $D_B \in \mathbb{R}^{m \times \ell}$ , and  $D_G \in \mathbb{R}^{d \times n}$  are quasi-diagonal matrices<sup>1</sup>. We refer the reader to [32] for detailed proof of the above decomposition.

<sup>1</sup>A quasi-diagonal matrix, in this work, is a matrix that is diagonal after removing all zero rows and columns.

Algorithms for the computation of the RSVD are still an active field of research; some recent works include [6, 33]. As noted in [8], the RSVD can be computed via a double GSVD. Following the formulation of the GSVD proposed by Van Loan [28]: Given  $A \in \mathbb{R}^{m \times n}$  and  $G \in \mathbb{R}^{d \times n}$  with  $m, d \geq n$ , there exist matrices  $U \in \mathbb{R}^{m \times m}$ ,  $V \in \mathbb{R}^{d \times d}$  with orthonormal columns and a nonsingular  $X \in \mathbb{R}^{n \times n}$  such that

$$(3.2) \quad \begin{aligned} U^T A X &= \Gamma = \text{diag}(\gamma_1, \dots, \gamma_n), & \gamma_i &\in [0, 1], \\ V^T G X &= \Sigma = \text{diag}(\sigma_1, \dots, \sigma_n), & \sigma_i &\in [0, 1], \end{aligned}$$

where  $\gamma_i^2 + \sigma_i^2 = 1$ . Let  $Y := X^{-T}$  in the GSVD of (3.2), then  $A = UTY^T$  and  $G = VSY^T$ . The following is a practical procedure to construct the RSVD using the GSVD. For ease of presentation, we first assume that  $m = \ell$  and  $d = n$  so that  $B$  and  $G$  are square. Then, we have the following expression as the RSVD from two GSVDs:

$$\begin{aligned} \begin{bmatrix} A & B \\ G & \end{bmatrix} &= \begin{bmatrix} U_1 & \\ & V_1 \end{bmatrix} \begin{bmatrix} \Gamma_1 & U_1^T B \\ \Sigma_1 & \end{bmatrix} \begin{bmatrix} Y_1^T \\ I \end{bmatrix} \\ &= \begin{bmatrix} U_1 & \\ & V_1 \end{bmatrix} \begin{bmatrix} \Gamma_1 \Sigma_1^{-1} & U_1^T B \\ I & \end{bmatrix} \begin{bmatrix} \Sigma_1 Y_1^T \\ I \end{bmatrix} \\ &= \begin{bmatrix} U_1 Y_2 & \\ & V_1 \end{bmatrix} \begin{bmatrix} \Sigma_2^T & \Gamma_2^T \\ V_2 & \end{bmatrix} \begin{bmatrix} V_2^T \Sigma_1 Y_1^T \\ U_2^T \end{bmatrix} \\ &= \begin{bmatrix} U_1 Y_2 & \\ & V_1 V_2 \end{bmatrix} \begin{bmatrix} \Sigma_2^T \Gamma_G & \Gamma_2^T \\ \Gamma_G & \end{bmatrix} \begin{bmatrix} Y_1 \Sigma_1 V_2 \Gamma_G^{-1} & \\ & U_2 \end{bmatrix}^T. \end{aligned}$$

The identity matrix is denoted by  $I$ . In these four steps, we have first computed the GSVD of  $(A, G)$ , i.e.,  $A = U_1 \Gamma_1 Y_1^T$  and  $G = V_1 \Sigma_1 Y_1^T$ . Note that  $\Sigma_1$  is nonsingular since  $G$  is nonsingular. Next, we compute the GSVD of the transposes of the pair  $(U_1^T B, \Gamma_1 \Sigma_1^{-1})$ , so that  $U_1^T B = Y_2 \Gamma_2^T U_2^T$  and  $\Gamma_1 \Sigma_1^{-1} = Y_2 \Sigma_2^T V_2^T$ . Moreover,  $\Gamma_G$  is a nonsingular scaling matrix that one can freely select (see, e.g., [33]). In this square case, we have  $\Sigma_2^T = \Sigma_2$ , but we keep this notation for consistency with the nonsquare case we will discuss now.

In some of our applications of interest (see [Experiments 5.3](#) and [5.4](#) in [section 5](#)), we have that  $\ell = d > m \geq n$ . In this case, we get the following modifications:

$$\begin{aligned} \begin{bmatrix} U_1 & \\ & V_1 \end{bmatrix} \begin{bmatrix} \Gamma_1 & U_1^T B \\ \Sigma_1 \\ 0_{d-n,n} \end{bmatrix} \begin{bmatrix} Y_1^T \\ I \end{bmatrix} \\ &= \begin{bmatrix} U_1 & \\ & V_1 \end{bmatrix} \begin{bmatrix} \Gamma_1 \Sigma_1^{-1} & U_1^T B \\ I \\ 0_{d-n,n} \end{bmatrix} \begin{bmatrix} \Sigma_1 Y_1^T \\ I \end{bmatrix} \\ &= \begin{bmatrix} U_1 Y_2 & \\ & V_1 \end{bmatrix} \begin{bmatrix} \Sigma_2^T & \Gamma_2^T \\ V_2 \\ 0_{d-n,n} \end{bmatrix} \begin{bmatrix} V_2^T \Sigma_1 Y_1^T \\ U_2^T \end{bmatrix} \\ &= \begin{bmatrix} U_1 Y_2 & \\ & V_1 \widehat{V}_2 \end{bmatrix} \begin{bmatrix} \Sigma_2^T \Gamma_G & \Gamma_2^T \\ \Gamma_G \\ 0_{d-n,n} \end{bmatrix} \begin{bmatrix} Y_1 \Sigma_1 V_2 \Gamma_G^{-1} & \\ & U_2 \end{bmatrix}^T. \end{aligned}$$

In these steps, we use  $\widehat{V}_2 = \text{diag}(V_2, I_{d-n})$ . In the two GSVD steps, we emphasize that we maintain the traditional nondecreasing ordering of the generalized singular values

in both GSVDs. That is, the diagonal entries of  $\Gamma_1$  and  $\Gamma_2$  are in nondecreasing order while those of  $\Sigma_1$  and  $\Sigma_2$  are in nonincreasing order. Note that  $\Sigma_1$  is again nonsingular because  $G$  is of full rank. With reference to (3.1), we define  $Z := U_1 Y_2$ ,  $W := Y_1 \Sigma_1 V_2 \Gamma_G^{-1}$ ,  $V := V_1 \widehat{V}_2$ ,  $U := U_2$ ,  $D_A := \Sigma_2^T \Gamma_G$ ,  $D_B := \Gamma_2^T$ , and  $D_G := \begin{bmatrix} \Gamma_G \\ 0_{d-n,n} \end{bmatrix}$ . The quasi-diagonal matrices  $D_A$  and  $D_B$  have the following structure:

$$(3.3) \quad D_A = \begin{bmatrix} D_1 \\ 0_{m-n,n} \end{bmatrix} \quad \text{and} \quad D_B = \begin{bmatrix} D_2 & & 0_{m,\ell-m} \\ & I_B & \end{bmatrix}.$$

Write  $\text{diag}(D_1) = (\alpha_1, \dots, \alpha_n)$ ,  $\text{diag}(D_2) = (\beta_1, \dots, \beta_n)$ ,  $\text{diag}(\Gamma_G) = (\gamma_1, \dots, \gamma_n)$  and  $\Sigma_2 = \text{diag}(\sigma_1, \dots, \sigma_n)$ , for  $i = 1, \dots, n$ . Note that, in view of the assumption that  $B$  and  $G$  are of full rank and  $m \geq n$ ,  $1 > \alpha_i \geq \alpha_{i+1} > 0$ ,  $1 > \gamma_i \geq \gamma_{i+1} > 0$ , and  $0 < \beta_i \leq \beta_{i+1} < 1$ .

As mentioned earlier,  $\Gamma_G$  is a scaling matrix one can freely choose. Given  $\Sigma_2$ , we may, for instance, choose  $\gamma_i = \frac{\sigma_i}{\sqrt{\sigma_i^2 + 1}}$ , which are nonzero and ordered nonincreasingly (since the function  $t \mapsto t(t^2 + 1)^{-1/2}$  is strictly increasing). This implies that  $\alpha_i = \frac{\sigma_i^2}{\sqrt{\sigma_i^2 + 1}}$ . Given that  $\beta_i^2 + \sigma_i^2 = 1$  from the second GSVD, we have that  $\alpha_i^2 + \beta_i^2 + \gamma_i^2 = 1$  for  $i = 1, \dots, n$ . Note that  $\frac{\alpha_i}{\beta_i \gamma_i} \geq \frac{\alpha_{i+1}}{\beta_{i+1} \gamma_{i+1}}$ , which follows from the fact that  $\alpha_i / \gamma_i = \sigma_i$ , which is nonincreasing.

We now state a connection of the RSVD with CCA. In [8], De Moor and Golub show a relation of the RSVD to a generalized eigenvalue problem. The related generalized eigenvalue problem of the RSVD of the matrix triplet  $(G^T B, G^T, B)$  with  $m = d$  as shown in [8, Sec. 2.2] is

$$\begin{bmatrix} & G^T B \\ B^T G & \end{bmatrix} \begin{bmatrix} \mathbf{z} \\ \mathbf{w} \end{bmatrix} = \lambda \begin{bmatrix} G^T G & \\ & B^T B \end{bmatrix} \begin{bmatrix} \mathbf{z} \\ \mathbf{w} \end{bmatrix}.$$

It is clear that the above problem is exactly the generalized eigenvalue problem of the  $\text{cca}(B, G)$ ; see (2.2) in section 2. Note that matrices  $B^T B$  and  $G^T G$  can be interpreted as covariance matrices. In applications where these covariance matrices are (almost) singular, one may use the RSVD instead to find a solution without explicitly solving the generalized eigenvalue problem.

**4. A Restricted SVD based CUR Decomposition and its Approximation Properties.** In this section, we describe the proposed RSVD-CUR decomposition and provide theoretical bounds on its approximation errors. We denote the pseudoinverse of  $C$  by  $C^+$  and use MATLAB notations to index vectors and matrices, i.e.,  $A(:, \mathbf{p})$  denotes the  $k$  columns of  $A$  with corresponding indices in vector  $\mathbf{p} \in \mathbb{N}_+^k$ .

**4.1. A Restricted SVD based CUR decomposition.** We now introduce a new RSVD-CUR decomposition of a matrix triplet  $(A, B, G)$  with  $A \in \mathbb{R}^{m \times n}$  (where, without loss of generality,  $m \geq n$ ),  $B \in \mathbb{R}^{m \times \ell}$ , and  $G \in \mathbb{R}^{d \times n}$  where  $B$  and  $G$  are of full rank. Table 1 in section 5 gives an overview of the various sizes of  $m$ ,  $n$ ,  $\ell$ , and  $d$  in the applications that we consider. This RSVD-CUR factorization is guided by the knowledge of the RSVD for matrix triplets reviewed in section 3. We now define a rank- $k$  RSVD-CUR approximation; cf. (1.1).

**DEFINITION 4.1.** *Let  $A$  be  $m \times n$ ,  $B$  be  $m \times \ell$ , and  $G$  be  $d \times n$ . A rank- $k$  RSVD-*

CUR approximation of  $(A, B, G)$  is defined as

$$(4.1) \quad \begin{aligned} A &\approx A_k := C_A M_A R_A := AP M_A S^T A, \\ B &\approx B_k := C_B M_B R_B := BP_B M_B S^T B, \\ G &\approx G_k := C_G M_G R_G := GP M_G S_G^T G. \end{aligned}$$

Here  $S \in \mathbb{R}^{m \times k}$ ,  $S_G \in \mathbb{R}^{d \times k}$ ,  $P \in \mathbb{R}^{n \times k}$ , and  $P_B \in \mathbb{R}^{\ell \times k}$  ( $k \leq \min(m, n, d, \ell)$ ) are index selection matrices with some columns of the identity that select rows and columns of the respective matrices.

It is key that *the same* rows of  $A$  and  $B$  are picked and *the same* columns of  $A$  and  $G$  are selected; this gives a coupling among the decompositions. The matrices  $C_A \in \mathbb{R}^{m \times k}$ ,  $C_B \in \mathbb{R}^{m \times k}$ ,  $C_G \in \mathbb{R}^{d \times k}$ , and  $R_A \in \mathbb{R}^{k \times n}$ ,  $R_B \in \mathbb{R}^{k \times \ell}$ ,  $R_G \in \mathbb{R}^{k \times n}$  are subsets of the columns and rows, respectively, of the given matrices. Let the vectors  $\mathbf{s}$ ,  $\mathbf{s}_G$ ,  $\mathbf{p}$ , and  $\mathbf{p}_B$  contain the indices of the selected rows and columns, so that  $S = I(:, \mathbf{s})$ ,  $S_G = I(:, \mathbf{s}_G)$ ,  $P = I(:, \mathbf{p})$ , and  $P_B = I(:, \mathbf{p}_B)$ . The choice of  $\mathbf{s}$ ,  $\mathbf{s}_G$ ,  $\mathbf{p}$ , and  $\mathbf{p}_B$  is guided by the knowledge of the orthogonal and nonsingular matrices from the rank- $k$  RSVD. Given the column and row index vectors, following [25, 22, 26], we compute the middle matrices as mentioned in section 1, that is,  $M_A = (C_A^T C_A)^{-1} C_A^T A R_A^T (R_A R_A^T)^{-1}$ , and similarly for  $M_B$  and  $M_G$ . There are several index selection strategies proposed in the literature for finding the “best” row and column indices. The approaches we employ are the DEIM [4] and the Q-DEIM [9] algorithms, which are greedy deterministic procedures and simple to implement.

The DEIM procedure has first been introduced in the context of model reduction of nonlinear dynamical systems [4]; it is a discrete variant of empirical interpolation proposed in [2]. Sorensen and Embree later show how the DEIM algorithm is a viable column and row index selection procedure for constructing a CUR factorization [25]. To construct  $C$  and  $R$ , apply the DEIM scheme to the top  $k$  right and left singular vectors, respectively [25]. The DEIM procedure uses a locally optimal projection technique similar to the pivoting strategy of the LU factorization. The column and row indices are selected by processing the singular vectors sequentially as summarized in Algorithm 4.1<sup>2</sup>. In [9], the authors propose a QR-factorization based DEIM called Q-DEIM, which is much simpler than the original DEIM and enjoys a sharper error bound for the DEIM projection error. The availability of the pivoted QR implementation in many open-source packages makes this algorithm an efficient alternative index selection scheme. Thus, Algorithm 4.2 can replace the DEIM algorithm to select the column and row indices.

---

**Algorithm 4.1** Discrete empirical interpolation index selection method (deim) [4]

---

**Require:**  $U \in \mathbb{R}^{m \times k}$  with  $k \leq m$  (full rank)

**Ensure:** Indices  $\mathbf{s} \in \mathbb{N}_+^k$  with non-repeating entries

```

1:  $\mathbf{s}(1) = \operatorname{argmax}_{1 \leq i \leq m} |(U(:, 1))_i|$ 
2: for  $j = 2, \dots, k$  do
3:    $U(:, j) = U(:, j) - U(:, 1:j-1) \cdot (U(\mathbf{s}, 1:j-1) \setminus U(\mathbf{s}, j))$ 
4:    $\mathbf{s}(j) = \operatorname{argmax}_{1 \leq i \leq m} |(U(:, j))_i|$ 
5: end for
```

---

The DEIM type CUR decomposition requires singular vectors or approximate singular vectors. In this paper, we apply the DEIM procedure to the nonsingular and

---

<sup>2</sup>The backslash operator used in the algorithms is a Matlab type notation for solving linear systems and least-squares problems.



**Algorithm 4.2** Q-DEIM index selection scheme [9]**Require:**  $U \in \mathbb{R}^{m \times k}$  with  $k \leq m$  (full rank)**Ensure:** Indices  $\mathbf{s} \in \mathbb{N}_+^k$  with non-repeating entries

- 1:  $[q, r, \text{pivot}] = \text{qr}(U^T)$  (perform column-pivoted QR on  $U$  transpose)
- 2:  $\mathbf{s} = \text{pivot}(1 : k)$

orthogonal matrices from the RSVD instead. In an SVD-based CUR factorization, the left and right singular vectors serve as bases for the column and row spaces of matrix  $A$ , respectively. In our new context, the columns of matrices  $Z$  and  $W$  from (3.1) may be viewed as bases for the column and row spaces, respectively, of  $A$  relative to the column space of  $B$  and the row space of  $G$ . The procedure for constructing a DEIM type RSVD-CUR is summarized in Algorithm 4.3. In Line 1, the columns of  $W$ ,  $Z$ ,  $U$ , and  $V$  corresponds to the  $k$  largest restricted singular values.

**Algorithm 4.3** DEIM type RSVD-CUR decomposition**Require:**  $A \in \mathbb{R}^{m \times n}$ ,  $B \in \mathbb{R}^{m \times \ell}$ ,  $G \in \mathbb{R}^{d \times n}$ , desired rank  $k$ **Ensure:** A rank- $k$  RSVD-CUR decomposition

- $$A_k = A(:, \mathbf{p}) \cdot M_A \cdot A(\mathbf{s}, :), \quad B_k = B(:, \mathbf{p}_B) \cdot M_B \cdot B(\mathbf{s}, :), \quad G_k = G(:, \mathbf{p}) \cdot M_G \cdot G(\mathbf{s}_G, :)$$
- 1: Compute rank- $k$  RSVD of  $(A, B, G)$  to obtain  $W, Z, U, V$  (see (3.1))
  - 2:  $\mathbf{p} = \text{deim}(W)$  (perform DEIM on the matrices from the RSVD)
  - 3:  $\mathbf{s} = \text{deim}(Z)$
  - 4:  $\mathbf{p}_B = \text{deim}(U)$
  - 5:  $\mathbf{s}_G = \text{deim}(V)$
  - 6:  $M_A = A(:, \mathbf{p}) \setminus (A / A(\mathbf{s}, :))$ ,  $M_B = B(:, \mathbf{p}_B) \setminus (B / B(\mathbf{s}, :))$ ,  
 $M_G = G(:, \mathbf{p}) \setminus (G / G(\mathbf{s}_G, :))$

In many applications, as we will see in section 5, one is interested in selecting only the key columns or rows and not the explicit  $A \approx C_A M_A R_A$  factorization. An interpolative decomposition aims to identify a set of skeleton columns or rows of a matrix. A CUR factorization may be viewed as evaluating the ID for both the column and row spaces of a matrix simultaneously. The following are the column and row versions of an RSVD-ID factorization of a matrix triplet:

$$\begin{aligned} A &\approx C_A \widetilde{M}_A, & B &\approx C_B \widetilde{M}_B, & G &\approx C_G \widetilde{M}_G, & \text{or} \\ A &\approx \widehat{M}_A R_A, & B &\approx \widehat{M}_B R_B, & G &\approx \widehat{M}_G R_G. \end{aligned}$$

Here,  $\widetilde{M}_A = C_A^+ A$  is  $k \times n$  and  $\widehat{M}_A = A R_A^+$  is  $m \times k$ ; analogous remarks hold for  $\widetilde{M}_B$ ,  $\widetilde{M}_G$ ,  $\widehat{M}_B$ , and  $\widehat{M}_G$ . Notice that in Algorithm 4.3, the key column and row indices of the various matrices are picked independently. This algorithm can therefore be restricted to select only column indices if we are interested in the column version of the RSVD-ID factorization or select only row indices if we are interested in the row version.

De Moor and Golub [8] show the relation between the RSVD and the SVD and its other generalizations. We indicate in the following proposition the corresponding connection between the DEIM type RSVD-CUR and the (generalized) CUR decomposition [25, 12].

**PROPOSITION 4.2.** (i) *If  $B$  and  $G$  are nonsingular matrices, then the selected row and column indices from a CUR decomposition of  $B^{-1}AG^{-1}$  are the same as index vectors  $\mathbf{p}_B$  and  $\mathbf{s}_G$ , respectively, obtained from an RSVD-CUR decomposition of  $(A, B, G)$ .*



(ii) Furthermore, in the particular case where  $B = I$  and  $G = I$ , the RSVD-CUR decomposition of  $A$  coincides with a CUR decomposition of  $A$ , in that the factors  $C$  and  $R$  of  $A$  are the same for both methods: the first line of (4.1) is equal to (1.1).

(iii) Lastly, given a special choice of  $B = I$ , an RSVD-CUR decomposition of  $A$  and  $G$  coincides with the GCUR decomposition of  $(A, G)$  (see [12, Def. 4.1]), in that the factors  $C_A, C_G$  and  $R_A, R_G$  of  $A$  and  $G$  are the same for both methods. In the dual case that instead of  $B, G = I$ , similar remarks hold.

*Proof.* (i) We start with the RSVD (3.1). If  $B$  and  $G$  are nonsingular, then the SVD of  $B^{-1}AG^{-1}$  can be expressed in terms of the RSVD of  $(A, B, G)$ , and is equal to  $U(D_B^{-1}D_AD_G^{-1})V^T$  given that  $B^{-1} = UD_B^{-1}Z^{-1}$  and  $G^{-1} = W^{-T}D_G^{-1}V^T$  [8]. Consequently, the row and column index vectors from a CUR factorization of  $B^{-1}AG^{-1}$  are equal to the vectors  $\mathbf{s}_G$  and  $\mathbf{p}_B$ , respectively, from an RSVD-CUR of  $(A, B, G)$  since they are obtained by applying DEIM to matrices  $V$  and  $U$ , respectively.

(ii) If  $B = I$  and  $G = I$ , from (3.1),  $I = ZD_BU^T$  and  $I = VD_GW^T$  which implies  $UD_B^{-1} = Z$  and  $W^T = D_G^{-1}V^T$ . Hence, we find that  $A = UD_B^{-1}D_AD_G^{-1}V^T$  which is an SVD of  $A$ . Therefore the selection matrices  $P, S$  from CUR of  $A$  (1.1) are equal to the selection matrices  $P_B, S_G$  from an RSVD-CUR of  $(A, I, I)$  (4.1).

(iii) If  $B = I$ , again from (3.1),  $I = ZD_BU^T$ , which implies  $UD_B^{-1} = Z$ . Then  $A = UD_B^{-1}D_AW^T, G = VD_GW^T$  which is (up to a diagonal scaling) the GSVD of the matrix pair  $(A, G)$ ; see (3.2) [8]. Thus, the column and row selection matrices from GCUR of  $(A, G)$  (see [12, Def. 4.1]) are the same as the column and row selection matrices  $P, S, S_G$  from (4.1), respectively.  $\square$

**4.2. Error Analysis.** We begin by analyzing the error of a rank- $k$  RSVD of a matrix triplet  $A \in \mathbb{R}^{m \times n}$  (where without loss of generality  $m \geq n$ ),  $B \in \mathbb{R}^{m \times \ell}$ , and  $G \in \mathbb{R}^{d \times n}$  (where  $B$  and  $G$  are of full rank). Given our applications of interest in section 5, we consider the case  $\ell = d \geq m \geq n$ . To define a rank- $k$  RSVD, let us partition the following matrices

$$U = [U_k \ \widehat{U}], \quad V = [V_k \ \widehat{V}], \quad W = [W_k \ \widehat{W}], \quad Z = [Z_k \ \widehat{Z}],$$

$$D_A = \text{diag}(D_{A_k}, \widehat{D}_A), \quad D_B = \text{diag}(D_{B_k}, \widehat{D}_B), \quad D_G = \text{diag}(D_{G_k}, \widehat{D}_G),$$

where  $\widehat{D}_A \in \mathbb{R}^{(m-k) \times (n-k)}$ ,  $\widehat{D}_B \in \mathbb{R}^{(m-k) \times (\ell-k)}$ , and  $\widehat{D}_G \in \mathbb{R}^{(d-k) \times (n-k)}$ . We define a rank- $k$  RSVD of  $(A, B, G)$  as

$$(4.2) \quad A_k := Z_k D_{A_k} W_k^T, \quad B_k := Z_k D_{B_k} U_k^T, \quad G_k := V_k D_{G_k} W_k^T,$$

where  $k < n$ . It follows that

$$(4.3) \quad A - A_k = \widehat{Z} \widehat{D}_A \widehat{W}^T, \quad B - B_k = \widehat{Z} \widehat{D}_B \widehat{U}^T, \quad G - G_k = \widehat{V} \widehat{D}_G \widehat{W}^T.$$

The following statements are a stepping stone for the error bound analysis of an RSVD-CUR. Denote the  $i$ -th singular value of  $A$  by  $\psi_i(A)$ . Let  $A - A_k = \widehat{Z} \widehat{D}_A \widehat{W}^T$  as in (4.3), then for  $i = 1, \dots, n$ ,  $\psi_i(\widehat{Z} \widehat{D}_A \widehat{W}^T) \leq \psi_i(\widehat{D}_A) \|\widehat{Z}\| \|\widehat{W}\|$  (see, e.g., [21, p. 346]). Since the diagonal elements of  $\widehat{D}_A$  are in nonincreasing order, we have  $\|A - A_k\| \leq \psi_1(\widehat{D}_A) \|\widehat{Z}\| \|\widehat{W}\| \leq \alpha_{k+1} \cdot \|\widehat{Z}\| \|\widehat{W}\|$ .

Similarly, we have that  $\|B - B_k\| = \|\widehat{Z} \widehat{D}_B \widehat{U}^T\| \leq \|\widehat{Z}\|$  and  $\|G - G_k\| = \|\widehat{V} \widehat{D}_G \widehat{W}^T\| \leq \gamma_{k+1} \cdot \|\widehat{W}\|$ . The first inequality follows from the fact  $\widehat{U}$  has orthonormal columns and the diagonal elements of  $\widehat{D}_B$  are in nondecreasing order with a maximum value of 1, so we have that  $\psi_1(\widehat{D}_B) = 1$  (see (3.3) for the structure of

$D_B$ ) and  $\|\widehat{U}\| = 1$ . The second equality is a result of the fact that  $\widehat{V}$  has orthonormal columns and the diagonal entries of  $\widehat{D}_G$  are in nonincreasing order, therefore,  $\psi_1(\widehat{D}_G) = \gamma_{k+1}$  and  $\|\widehat{V}\| = 1$ .

We now introduce some error bounds of an RSVD-CUR decomposition in terms of the error of a rank- $k$  RSVD. The analysis closely follows the error bound analysis in [25, 12] for the DEIM type CUR and DEIM type GCUR methods with some necessary modifications. As with the DEIM type GCUR method, here also, the lack of orthogonality of the vectors in  $W$  and  $Z$  from the RSVD necessitates some additional work. We take a QR factorization of  $W$  and  $Z$  to obtain an orthonormal basis to facilitate the analysis, introducing terms in the error bound associated with the triangular matrix in the QR factorization.

For the analysis, we use the following QR decomposition of the nonsingular matrices from the RSVD (see (3.1))

$$(4.4) \quad \begin{aligned} [Z_k \quad \widehat{Z}] &= Z = Q_Z T_Z = [Q_{Z_k} \quad \widehat{Q}_Z] \begin{bmatrix} T_{Z_k} & T_{Z_{12}} \\ 0 & T_{Z_{22}} \end{bmatrix} = [Q_{Z_k} T_{Z_k} \quad Q_Z \widehat{T}_Z], \\ [W_k \quad \widehat{W}] &= W = Q_W T_W = [Q_{W_k} \quad \widehat{Q}_W] \begin{bmatrix} T_{W_k} & T_{W_{12}} \\ 0 & T_{W_{22}} \end{bmatrix} = [Q_{W_k} T_{W_k} \quad Q_W \widehat{T}_W], \end{aligned}$$

where we have defined

$$(4.5) \quad \widehat{T}_Z := \begin{bmatrix} T_{Z_{12}} \\ T_{Z_{22}} \end{bmatrix}, \quad \widehat{T}_W := \begin{bmatrix} T_{W_{12}} \\ T_{W_{22}} \end{bmatrix}.$$

This implies that

$$(4.6) \quad \begin{aligned} A &= A_k + \widehat{Z} \widehat{D}_A \widehat{W}^T = Z_k D_{A_k} W_k^T + \widehat{Z} \widehat{D}_A \widehat{W}^T \\ &= Q_{Z_k} T_{Z_k} D_{A_k} T_{W_k}^T Q_{W_k}^T + Q_Z \widehat{T}_Z \widehat{D}_A \widehat{T}_W^T Q_W^T, \\ B &= B_k + \widehat{Z} \widehat{D}_B \widehat{U}^T = Z_k D_{B_k} U_k^T + \widehat{Z} \widehat{D}_B \widehat{U}^T = Q_{Z_k} T_{Z_k} D_{B_k} U_k^T + Q_Z \widehat{T}_Z \widehat{D}_B \widehat{U}^T, \\ G &= G_k + \widehat{V} \widehat{D}_G \widehat{W}^T = V_k D_{G_k} W_k^T + \widehat{V} \widehat{D}_G \widehat{W}^T = V_k D_{G_k} T_{W_k}^T Q_{W_k}^T + \widehat{V} \widehat{D}_G \widehat{T}_W^T Q_W^T. \end{aligned}$$

Given an orthonormal matrix  $Q_W \in \mathbb{R}^{n \times k}$ , from [25, 12] as well as here, we have that the quantity  $\|A(I - Q_{W_k} Q_{W_k}^T)\|$  is key in the error bound analysis. Here, we have that  $\|A(I - Q_{W_k} Q_{W_k}^T)\|$  may not be close to  $\psi_k(A)$  since the matrix  $Q_{W_k}$  is from the RSVD, therefore we provide a bound on this quantity in terms of the error in the RSVD.

Let  $P$  be an index selection matrix derived from performing the DEIM scheme on matrix  $W_k$ . Suppose  $Q_{W_k}$  is an orthonormal basis for  $\text{Range}(W_k)$ , with  $W_k^T P$  and  $Q_{W_k}^T P$  being nonsingular, we have the interpolatory projector  $P(W_k^T P)^{-1} W_k^T = P(Q_{W_k}^T P)^{-1} Q_{W_k}^T$  (see [4, Def. 3.1, Eq. 3.6]). With this equality, we exploit the special properties of an orthogonal matrix by using the orthonormal basis of the nonsingular matrices from the RSVD instead for our analysis. Let  $Q_{W_k}^T P$  and  $S^T Q_{Z_k}$  be nonsingular so that  $\mathbb{P} = P(Q_{W_k}^T P)^{-1} Q_{W_k}^T$  and  $\mathbb{S} = Q_{Z_k} (S^T Q_{Z_k})^{-1} S^T$ ; oblique projectors.

In the following theorem, we provide bounds on the coupled CUR decompositions of  $A$ ,  $B$ , and  $G$  in terms of the RSVD quantities. The upper bounds contain both multiplicative factors (the  $\eta$ 's) and the  $\alpha_{k+1}$ ,  $\gamma_{k+1}$  (both bounded by 1), and  $T$ -quantities, which are from the error of the truncated RSVD as defined in (4.2) and (4.3).

**THEOREM 4.3.** (Generalization of [25, Thm. 4.1] and [12, Thm. 4.8]) Given  $A$ ,  $B$ , and  $G$  as in Definition 4.1 and  $Z_k \in \mathbb{R}^{m \times k}$ ,  $W_k \in \mathbb{R}^{n \times k}$ ,  $U_k \in \mathbb{R}^{\ell \times k}$ , and  $V_k \in \mathbb{R}^{d \times k}$  from (4.2), let  $Q_{Z_k} \in \mathbb{R}^{m \times k}$ ,  $Q_{W_k} \in \mathbb{R}^{n \times k}$  be the  $Q$ -factors of  $Z_k, W_k$ , respectively, and  $\widehat{T}_Z, T_{Z_{22}}, \widehat{T}_W$ , and  $T_{W_{22}}$  as in (4.4)–(4.5). Suppose  $Q_{W_k}^T P, U_k^T P_B, S_G^T V_k$ , and  $S^T Q_{Z_k}$  are nonsingular, then with the error constants

$$\eta_p := \|(Q_{W_k}^T P)^{-1}\|, \quad \eta_s := \|(S^T Q_{Z_k})^{-1}\|, \quad \eta_{p_B} := \|(U_k^T P_B)^{-1}\|, \quad \eta_{s_G} := \|(S_G^T V_k)^{-1}\|,$$

we have

$$(4.7) \quad \begin{aligned} \|A - C_A M_A R_A\| &\leq \alpha_{k+1} \cdot (\eta_p \cdot \|\widehat{T}_Z\| \|T_{W_{22}}\| + \eta_s \cdot \|T_{Z_{22}}\| \|\widehat{T}_W\|) \\ &\leq \alpha_{k+1} \cdot (\eta_p + \eta_s) \cdot \|\widehat{T}_W\| \|\widehat{T}_Z\|, \\ \|B - C_B M_B R_B\| &\leq \eta_{p_B} \cdot \|T_{Z_{22}}\| + \eta_s \cdot \|\widehat{T}_Z\| \leq (\eta_{p_B} + \eta_s) \cdot \|\widehat{T}_Z\|, \\ \|G - C_G M_G R_G\| &\leq \gamma_{k+1} \cdot (\eta_p \cdot \|\widehat{T}_W\| + \eta_{s_G} \cdot \|T_{W_{22}}\|) \leq \gamma_{k+1} \cdot (\eta_p + \eta_{s_G}) \cdot \|\widehat{T}_W\|. \end{aligned}$$

*Proof.* We will prove the result for  $\|A - C_A M_A R_A\|$  in Theorem 4.3; the results for  $\|B - C_B M_B R_B\|$  and  $\|G - C_G M_G R_G\|$  follow similarly. We first show the bounds on the errors between  $A$  and its interpolatory projections  $\mathbb{P}A$  and  $A\mathbb{S}$ , i.e., the selected rows and columns. Then, using the fact that these bounds also apply to the orthogonal projections of  $A$  onto the same columns and rows spaces [25, Lemma 4.2], we prove the bound on the approximation of  $A$  by an RSVD-CUR.

Given the projector  $\mathbb{P}$ , we have that  $Q_{W_k}^T \mathbb{P} = Q_{W_k}^T P (Q_{W_k}^T P)^{-1} Q_{W_k}^T = Q_{W_k}^T$ , which implies  $Q_{W_k}^T (I - \mathbb{P}) = 0$ . Therefore the error in the oblique projection of  $A$  is (cf. [25, Lemma 4.1])

$$\begin{aligned} \|A - A\mathbb{P}\| &= \|A(I - \mathbb{P})\| = \|A(I - Q_{W_k} Q_{W_k}^T)(I - \mathbb{P})\| \\ &\leq \|A(I - Q_{W_k} Q_{W_k}^T)\| \|I - \mathbb{P}\|. \end{aligned}$$

Note that, since  $k < n$ ,  $\mathbb{P} \neq 0$  and  $\mathbb{P} \neq I$ , it is well known that (see, e.g., [27])

$$\|I - \mathbb{P}\| = \|\mathbb{P}\| = \|(Q_{W_k}^T P)^{-1}\|.$$

Using the partitioning of  $A$  in (4.6), we have

$$\begin{aligned} A Q_{W_k} Q_{W_k}^T &= [Q_{Z_k} \quad \widehat{Q}_Z] \begin{bmatrix} T_{Z_k} & T_{Z_{12}} \\ 0 & T_{Z_{22}} \end{bmatrix} \begin{bmatrix} D_{A_k} & 0 \\ 0 & \widehat{D}_A \end{bmatrix} \begin{bmatrix} T_{W_k}^T & 0 \\ T_{W_{12}}^T & T_{W_{22}}^T \end{bmatrix} \begin{bmatrix} I_k \\ 0 \end{bmatrix} Q_{W_k}^T \\ &= Q_{Z_k} T_{Z_k} D_{A_k} T_{W_k}^T Q_{W_k}^T + Q_Z \widehat{T}_Z \widehat{D}_A T_{W_{12}}^T Q_{W_k}^T, \end{aligned}$$

and hence

$$\begin{aligned} A(I - Q_{W_k} Q_{W_k}^T) &= (A - A_k) - Q_Z \widehat{T}_Z \widehat{D}_A T_{W_{12}}^T Q_{W_k}^T \\ &= Q_Z \widehat{T}_Z \widehat{D}_A \widehat{T}_W^T Q_W^T - Q_Z \widehat{T}_Z \widehat{D}_A T_{W_{12}}^T Q_{W_k}^T = Q_Z \widehat{T}_Z \widehat{D}_A T_{W_{22}}^T \widehat{Q}_W^T. \end{aligned}$$

This implies

$$\|A(I - Q_{W_k} Q_{W_k}^T)\| \leq \|\widehat{D}_A\| \|\widehat{T}_Z\| \|T_{W_{22}}\| \leq \alpha_{k+1} \cdot \|\widehat{T}_Z\| \|T_{W_{22}}\|,$$

and

$$\|A(I - \mathbb{P})\| \leq \alpha_{k+1} \cdot \|(Q_{W_k}^T P)^{-1}\| \|\widehat{T}_Z\| \|T_{W_{22}}\|.$$

Let us now consider the operation on the left side of  $A$ . Given that  $S^T Q_{Z_k}$  is nonsingular, we have the DEIM interpolatory projector  $\mathbb{S} = Q_{Z_k} (S^T Q_{Z_k})^{-1} S^T$ . It is known that (see [25, Lemma 4.1])

$$\begin{aligned} \|A - \mathbb{S}A\| &= \|(I - \mathbb{S})A\| = \|(I - \mathbb{S})(I - Q_{Z_k} Q_{Z_k}^T)A\| \\ &\leq \|(I - \mathbb{S})\| \|(I - Q_{Z_k} Q_{Z_k}^T)A\|. \end{aligned}$$

Similar to before, since  $k < m$ , we know that  $\mathbb{S} \neq 0$  and  $\mathbb{S} \neq I$  hence

$$\|I - \mathbb{S}\| = \|\mathbb{S}\| = \|(S^T Q_{Z_k})^{-1}\|.$$

In the same setting as earlier, we have the following expansion

$$\begin{aligned} Q_{Z_k} Q_{Z_k}^T A &= [Q_{Z_k} \ 0] \begin{bmatrix} T_{Z_k} & T_{Z_{12}} \\ 0 & T_{Z_{22}} \end{bmatrix} \begin{bmatrix} D_{A_k} & 0 \\ 0 & \hat{D}_A \end{bmatrix} \begin{bmatrix} T_{W_k}^T & 0 \\ T_{W_{12}}^T & T_{W_{22}}^T \end{bmatrix} \begin{bmatrix} Q_{W_k}^T \\ \hat{Q}_W^T \end{bmatrix} \\ &= Q_{Z_k} T_{Z_k} D_{A_k} T_{W_k}^T Q_{W_k}^T + Q_{Z_k} T_{Z_{12}} \hat{D}_A \hat{T}_W^T Q_W^T. \end{aligned}$$

We observe that

$$\begin{aligned} (I - Q_{Z_k} Q_{Z_k}^T)A &= (A - A_k) - Q_{Z_k} T_{Z_{12}} \hat{D}_A \hat{T}_W^T Q_W^T \\ &= Q_Z \hat{T}_Z \hat{D}_A \hat{T}_W^T Q_W^T - Q_{Z_k} T_{Z_{12}} \hat{D}_A \hat{T}_W^T Q_W^T = \hat{Q}_Z T_{Z_{22}} \hat{D}_A \hat{T}_W^T Q_W^T. \end{aligned}$$

Consequently,

$$\begin{aligned} \|(I - Q_{Z_k} Q_{Z_k}^T)A\| &= \|\hat{Q}_Z T_{Z_{22}} \hat{D}_A \hat{T}_W^T Q_W^T\| \leq \|\hat{D}_A\| \|T_{Z_{22}}\| \|\hat{T}_W\| \\ &\leq \alpha_{k+1} \cdot \|T_{Z_{22}}\| \|\hat{T}_W\|, \end{aligned}$$

and

$$\|(I - \mathbb{S})A\| \leq \alpha_{k+1} \cdot \|(S^T Q_{Z_k})^{-1}\| \|T_{Z_{22}}\| \|\hat{T}_W\|.$$

Suppose that  $C_A$  and  $R_A$  are of full rank, given the orthogonal projectors  $C_A C_A^+$  and  $R_A^+ R_A$  and computing  $M_A$  as  $(C_A^T C_A)^{-1} C_A^T A R_A^T (R_A R_A^T)^{-1} = C_A^+ A R_A^+$ , we have (see [22, Eq. 6])

$$A - C_A M_A R_A = A - C_A C_A^+ A R_A^+ R_A = (I - C_A C_A^+)A + C_A C_A^+ A (I - R_A^+ R_A).$$

Using the triangle inequality, it follows that [25, Lemma 4.2]

$$\|A - C_A M_A R_A\| = \|A - C_A C_A^+ A R_A^+ R_A\| \leq \|(I - C_A C_A^+)A\| + \|C_A C_A^+\| \|A(I - R_A^+ R_A)\|.$$

Leveraging the fact that  $C_A C_A^+$  is an orthogonal projector so  $\|C_A C_A^+\| = 1$ , and [25, Lemma 4.2]

$$\|(I - C_A C_A^+)A\| \leq \|A(I - \mathbb{P})\|, \quad \|A(I - R_A^+ R_A)\| \leq \|(I - \mathbb{S})A\|,$$

as a variant of [12, Thm. 4.8] we have

$$\begin{aligned} \|A - C_A M_A R_A\| &\leq \alpha_{k+1} \cdot (\|\hat{T}_Z\| \|T_{W_{22}}\| \|(Q_{W_k}^T P)^{-1}\| + \|(S^T Q_{Z_k})^{-1}\| \|T_{Z_{22}}\| \|\hat{T}_W\|) \\ &\leq \alpha_{k+1} \cdot (\|(Q_{W_k}^T P)^{-1}\| + \|(S^T Q_{Z_k})^{-1}\|) \cdot \|\hat{T}_Z\| \|\hat{T}_W\|. \end{aligned}$$

The last inequality follows directly from the fact that the norms of the submatrices of  $\hat{T}_{Z_{22}}$  and  $\hat{T}_{W_{22}}$  are at most  $\|\hat{T}_Z\|$  and  $\|\hat{T}_W\|$ , respectively.  $\square$

**Theorem 4.3** suggests that to keep the approximation errors as small as possible, a good index selection procedure that provides smaller quantities  $\|(U_k^T P_B)^{-1}\|$ ,  $\|(S_G^T V_k)^{-1}\|$ ,  $\|(Q_{W_k}^T P)^{-1}\|$ , and  $\|(S^T Q_{Z_k})^{-1}\|$  would be ideal. The DEIM procedure may be seen as an attempt to attain exactly that. Meanwhile, the quantity  $\alpha_{k+1} \cdot \|\widehat{T}_Z\| \|\widehat{T}_W\|$  is a result of the error of the rank- $k$  RSVD. Additionally, we would like to point out that due to the connection of QDEIM with strong rank-revealing QR factorization (matrix volume maximization), the upper bounds for the error constants can be reduced to the theoretically best available one if the QDEIM procedure for the selection of the indices is used instead of the DEIM algorithm [9, 10].

Comparing the results of the decomposition of  $A$  in **Theorem 4.3** to [25, Thm. 4.1], we have that the  $\sigma_{k+1}$  in [25, Thm. 4.1] is replaced by the error in the RSVD through  $\|(I - Q_{Z_k} Q_{Z_k}^T)A\|$  and  $\|A(I - Q_{W_k} Q_{W_k}^T)\|$ . Here,  $\|(Q_{W_k}^T P)^{-1}\|$ , and  $\|(S^T Q_{Z_k})^{-1}\|$  are computed using the orthonormal basis of the nonsingular matrices from the RSVD of  $A$  rather than the singular vectors. Compared with the results in [12, Thm. 4.8] where all quantities are a result of the GSVD, in **Theorem 4.3** we have an additional  $\|\widehat{T}_Z\|$ , and all quantities are a result of the RSVD.

**5. Numerical Experiments.** In this section, we first evaluate the performance of the proposed RSVD-CUR decomposition for reconstructing a data matrix perturbed with nonwhite noise. We then show how the proposed algorithm can be used for feature selection in multi-view and multi-label classification problems. In **Experiments 5.3** and **5.4**, we only care about the key columns of  $B$  and  $G$  so we do not explicitly compute the RSVD-CUR factorization.

In **Experiments 5.1** and **5.2**, we consider two popular covariance structures [30] for the correlated noise. The first covariance matrix has a compound symmetry structure (CS), which means the covariance matrix has constant diagonal and constant off-diagonal entries. A homogeneous compound symmetry covariance matrix is of the form

$$(5.1) \quad \text{CS}_{\text{cov}} = \nu^2 \begin{bmatrix} 1 & \xi & \xi & \xi \\ & 1 & \xi & \xi \\ & & 1 & \xi \\ & & & 1 \end{bmatrix},$$

where  $\nu$  and  $\xi$  (with  $-1 < \xi < 1$ ) denote the variance and correlation coefficient, respectively. The second covariance matrix we use has a first-order autoregressive structure (AR(1)), which implies the matrix has a constant diagonal and the off-diagonal entries decaying exponentially; it assumes that the correlation between any two elements gets smaller the further apart they are separated (e.g., in terms of time or space). A homogeneous AR(1) covariance matrix is of the form

$$(5.2) \quad \text{AR}(1)_{\text{cov}} = \nu^2 \begin{bmatrix} 1 & \xi & \xi^2 & \xi^3 \\ & 1 & \xi & \xi^2 \\ & & 1 & \xi \\ & & & 1 \end{bmatrix}.$$

An overview of the various examples and sizes for  $A \in \mathbb{R}^{m \times n}$ ,  $B \in \mathbb{R}^{m \times \ell}$ , and  $G \in \mathbb{R}^{d \times n}$  considered in this section is provided in **Table 1**.

*Experiment 5.1.* For our first experiment, we consider a matrix perturbation problem of the form  $A_E = A + BFG$ , where  $F$  is a Gaussian random matrix and  $B, G$  are the Cholesky factors of two non-diagonal noise covariance matrices. The goal is to reconstruct a low-rank matrix  $A$  from  $A_E$  assuming that the noise covariance matrices or their estimates are known. The requirement that the noise covariance

TABLE 1  
*Various examples and dimensions considered.*

Exp.	Problem	Relations	$m$	$n$	$\ell$	$d$
1-2	Perturbation	$m = \ell, n = d$	10000	1000	10000	1000
3	Multiview	$\ell = d > m > n$	76	64	2000	2000
			240	76	2000	2000
			928	512	2386	2386
4	Multilabel	$\ell = d > m > n$	103	14	2417	2417
			1836	159	7395	7395
			2150	208	87856	87856

matrices or their estimates should be known is not always trivial. We evaluate and compare a rank- $k$  RSVD-CUR and CUR decomposition of  $A_E$  in terms of reconstructing matrix  $A$ . The approximation quality of each decomposition is assessed by the relative matrix approximation error, i.e.,  $\|A - \tilde{A}\| / \|A\|$ , where  $\tilde{A}$  is the reconstructed low-rank matrix.

As an adaptation of the first experiment in [25, Ex. 6.1] we generate a rank-100 sparse nonnegative matrix  $A \in \mathbb{R}^{10000 \times 1000}$  of the form

$$A = \sum_{j=1}^{10} \frac{2}{j} \mathbf{x}_j \mathbf{y}_j^T + \sum_{j=11}^{100} \frac{1}{j} \mathbf{x}_j \mathbf{y}_j^T,$$

where  $\mathbf{x}_j \in \mathbb{R}^{10000}$  and  $\mathbf{y}_j \in \mathbb{R}^{1000}$  are random sparse vectors with nonnegative entries (in Matlab,  $\mathbf{x}_j = \text{sprand}(10000, 1, 0.025)$  and  $\mathbf{y}_j = \text{sprand}(1000, 1, 0.025)$ ). We then perturb  $A$  with a nonwhite noise matrix  $BFG$  (see, e.g., [18, p. 55]). The matrix  $F \in \mathbb{R}^{10000 \times 1000}$  is random Gaussian noise. We assume that  $B \in \mathbb{R}^{10000 \times 10000}$  is the Cholesky factor of a symmetric positive definite covariance matrix with compound symmetry structure (5.1) (with diagonal entries 4 and off-diagonal entries 1), and  $G \in \mathbb{R}^{1000 \times 1000}$  is the Cholesky factor of a symmetric positive definite covariance matrix with first-order autoregressive structure (5.2) (with diagonal entries 1 and the off-diagonal entries related by a multiplicative factor of 0.99). The resulting perturbed matrix we use is of the form  $A_E = A + \varepsilon \frac{\|A\|}{\|BFG\|} BFG$ , where  $\varepsilon$  is the noise level.

Given a noise level, we compare the naive approaches (rank- $k$  SVD-based methods), which do not take the structure of the noise into account with the methods (rank- $k$  RSVD-based methods), which consider the actual noise. That is, we compute the SVD of  $A_E$  and the RSVD of  $(A_E, B, G)$  to obtain the input matrices for a CUR and an RSVD-CUR decomposition, respectively. For each noise level, we generate ten random cases and take the average of the relative errors for varying  $k$  values.

Figure 1 summarizes the results of three noise levels (0.1, 0.15, 0.2). We observe that to approximate  $A$ , the RSVD-CUR factorization enjoys a considerably lower average approximation error than the CUR decomposition. The error of the former is at least half of the latter. Meanwhile, the average relative error of an RSVD-CUR approximation unlike that of the RSVD (monotonically decreasing) approaches  $\varepsilon$  after a certain value of  $k$ . This situation is natural because the RSVD-CUR routine picks actual columns and rows of  $A_E$ , so the relative error is likely to be saturated by the noise. The rank- $k$  SVD of  $A_E$  fails in approximating  $A$  for the given values of  $k$ . Its average relative error rapidly approaches  $\varepsilon$ ; this is expected since the covariance of the noise is not a multiple of the identity. The truncated SVD of  $A_E$  gives the optimal rank- $k$  approximation to  $A_E$ . However, here, the goal is to reconstruct the noise-free matrix  $A$  hence, we measure the rank- $k$  approximation error against the unperturbed  $A$ . To heuristically explain why the SVD fails here, let us consider the

ideal situation of a perturbation matrix  $E$  whose entries are normally distributed with zero mean and standard deviation  $\nu$  (white noise). We have that the expected value of  $\|E\|$  is approximately  $\nu\sqrt{m}$  [18]. Hence if the singular values of unperturbed  $A$  decay gradually to zero, then the singular values of the perturbed matrix  $A_E$  are expected to decrease monotonically (by definition) until they tend to settle at a level  $\tau = \nu\sqrt{m}$  determined by the errors in  $A_E$  [18]. Note that given that the rank of  $A$  is  $k$ , the singular values ( $\psi_i$ ) of  $A_E$  will level at  $i = k + 1$ . We can therefore expect to estimate  $A$  in terms of the rank- $k$  SVD  $A_E$  [18]. In this experiment, given the structure of the noise  $E = BFG$ , the expected value of  $\|E\|$  is not approximately  $\nu\sqrt{m}$ . As a result, the rank- $k$  SVD of  $A_E$  fails to estimate  $A$ . We need algorithms that can take the actual noise into account, which is typically done by the “prewhitening” process. Thus, given the nonsingular error equilibration matrices  $B$  and  $G$ , we have that the error in  $B^{-1}A_E G^{-1}$  is equilibrated, i.e., uncorrelated with zero mean and equal variance (white noise). One may then approximate  $A$  by applying the truncated SVD to the matrix  $B^{-1}A_E G^{-1}$ , followed by a “dewhitening” by a means of left and right multiplication with  $B$  and  $G$ , respectively [18]. However, it is worth noting that even when  $B$  and  $G$  are nonsingular it is computationally risky to work with their inverses since they may be close to singular, and so in general it makes sense to reformulate the problem with no inverses. Using the RSVD formulation, this “prewhitening” and “dewhitening” process becomes an integral part of the algorithm.

Another observation worth pointing out is that a rank- $k$  CUR of  $A_E$  yields a more accurate approximation of  $A$  compared to the rank- $k$  SVD of  $A_E$ , although the column and row indices are selected using the singular vectors of  $A_E$ . This behavior may be attributed to the fact that unlike the SVD, which is a linear combination of the perturbed data points, the  $C$  and  $R$  are actual columns and rows of  $A$  that are perturbed. Therefore, it is highly likely that these selected columns and rows are not largely perturbed.

It is also worth noting that the improved performance of an RSVD-CUR approximation compared to a CUR factorization is particularly more attractive for higher noise levels with modest  $k$  values, i.e., when  $k$  is significantly less than  $\text{rank}(A)$ . One can observe from Figure 1 that the range of  $k$  values that yield the lowest approximation error measured against unperturbed  $A$  is between 10 and 20. Using the following  $k$  values [10,15,20], in Table 2, we investigate the significant improvement of a DEIM-RSVD-CUR approximation over a DEIM-CUR factorization. With noise level 0.1, we see that for the lowest error of the DEIM-CUR, which corresponds to  $k = 15$ , the DEIM-RSVD-CUR produces about 64% reduction in that error. The improvement is even more significant if the noise level is 0.2, where the rank-10 RSVD-CUR approximation reduces the rank-10 CUR decomposition error (lowest error of the CUR) by about 102%.

TABLE 2

*The approximation quality of RSVD-CUR approximations compared with CUR approximations in recovering a sparse, nonnegative matrix  $A$  perturbed with nonwhite noise. The average relative errors  $\|A - \tilde{A}_k\| / \|A\|$  for  $k$  values [10,15,20]*

Noise	Method \ k	10	15	20
$\varepsilon = 0.1$	CUR- $\tilde{A}_k$	0.100	0.084	0.089
	RSVD-CUR- $\tilde{A}_k$	0.064	0.051	0.049
$\varepsilon = 0.2$	CUR- $\tilde{A}_k$	0.162	0.177	0.184
	RSVD-CUR- $\tilde{A}_k$	0.080	0.084	0.106



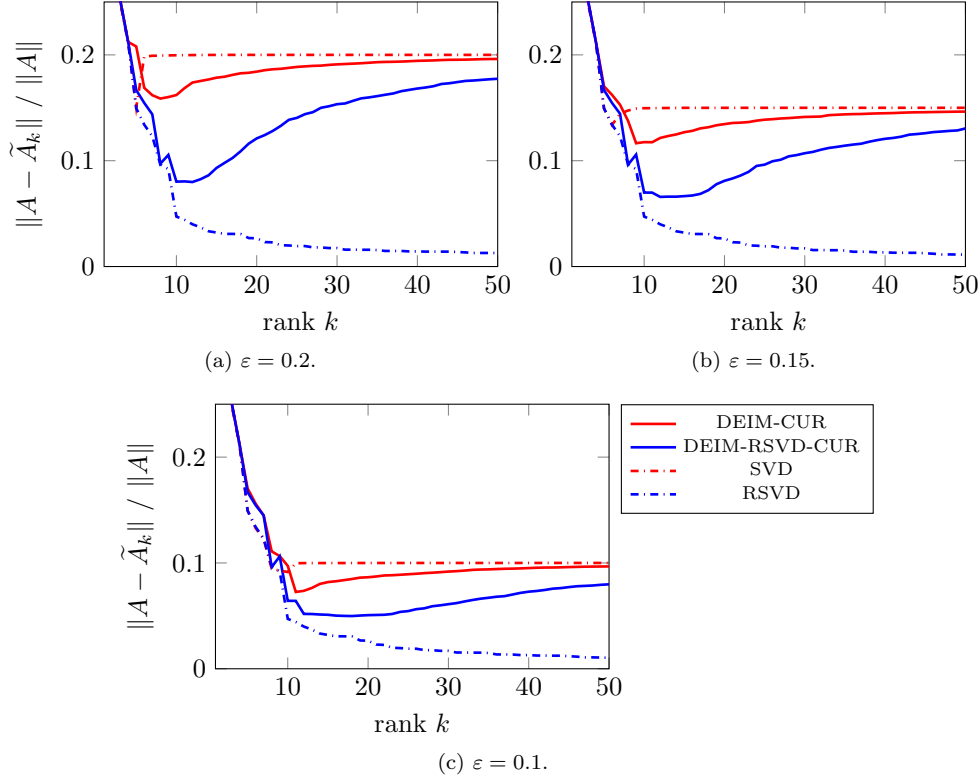


FIG. 1. The approximation quality of RSVD-CUR approximations compared with CUR approximations in recovering a sparse, nonnegative matrix  $A$  perturbed with nonwhite noise. The average relative errors  $\|A - \tilde{A}_k\| / \|A\|$  (on the vertical axis) as a function of rank  $k$  (on the horizontal axis) for  $\varepsilon = 0.2, 0.15, 0.1$ , respectively.

In Figure 2, using an RSVD-CUR decomposition of  $A_E$  with noise level  $\varepsilon = 0.1$ , we show the various quantities in Theorem 4.3. We observe that the upper bound in Theorem 4.3 may be rather pessimistic, and the true RSVD-CUR error may be substantially lower in practice. As in [25, Fig. 4], the magnitude of the quantities  $\eta_s$  and  $\eta_p$  may vary. We see that  $\|\hat{T}_W\|$  and  $\|\hat{T}_Z\|$  seem to stabilize as  $k$  increases and both quantities are close to  $\|A_E\|$ .

*Experiment 5.2.* In this experiment, we examine the case of using inexact Cholesky factors  $\hat{B}$  and  $\hat{G}$ . Suppose that given  $A_E$ , the exact noise covariance matrices  $B^T B$  and  $G^T G$  are unknown; we now investigate the approximation quality of the proposed RSVD-CUR decomposition compared with a CUR factorization in reconstructing  $A$  from  $A_E$ . We derive the inexact Cholesky factors  $\hat{B}$  and  $\hat{G}$  by multiplying the off-diagonal elements of the exact Cholesky factors  $B$  and  $G$  by uniform random numbers from the interval  $[0.9, 1.1]$ . Aside from the Cholesky factors, which we perturb here, we maintain the experimental setup described in Experiment 5.1 using noise levels  $\varepsilon = 0.1, 0.2$ ; the difference is that here we compute the RSVD of  $(A_E, \hat{B}, \hat{G})$  to get the input matrices for the RSVD-CUR decomposition. Figures 3a and 3b show that, when we use inexact Cholesky factors, the RSVD and RSVD-CUR factorization still deliver good approximation results, which may imply that we may not necessarily

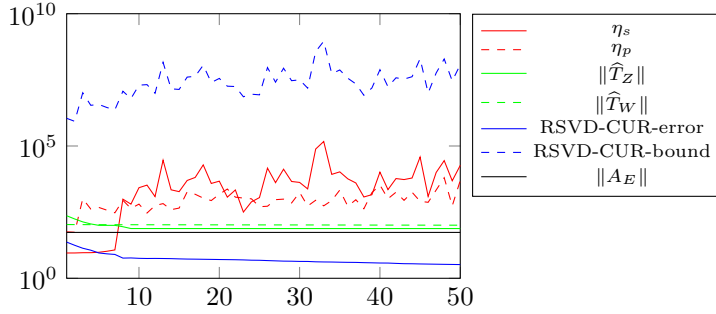


FIG. 2. First row: Various quantities from *Theorem 4.3*: error constants  $\eta_p = \|(Q_W^T P)^{-1}\|$  (red dashed) and  $\eta_s = \|(S_A^T Q_Z)^{-1}\|$  (red solid); multiplicative factors  $\|\hat{T}_Z\|$  (green solid) and  $\|\hat{T}_W\|$  (green dashed); an RSVD-CUR true error  $\|A_E - (CMR)_{\text{rsvd-cur}}\|$  of approximating  $A_E$  in *Experiment 5.1* (blue solid) and its upper bound (blue dashed).

need the exact noise covariance.

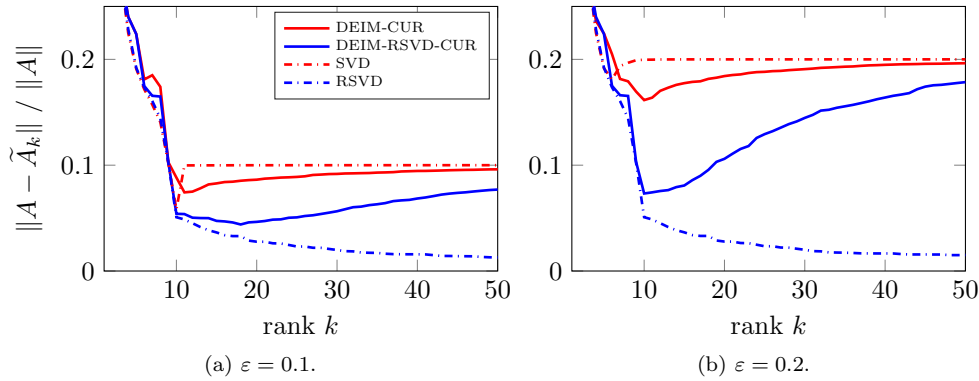


FIG. 3. The approximation quality of RSVD-CUR factorizations using inexact Cholesky factors of the noise covariance matrices compared with CUR decompositions in recovering a sparse, nonnegative matrix  $A$  perturbed with nonwhite noise. The average relative errors  $\|A - \tilde{A}_k\| / \|A\|$  (on the vertical axis) as a function of rank  $k$  (on the horizontal axis) for  $\varepsilon = 0.2, 0.1$ , respectively.

*Experiment 5.3.* In this experiment, we demonstrate the effectiveness of the proposed RSVD-CUR in discovering the underlying class structure shared by two views of a given data. We show that using the RSVD-CUR algorithm as a feature selection method in a multi-view classification problem can improve classification accuracy. Multi-view classification problems generally focus on classification accuracy by using information from different views, typically by integrating them into a unified, comprehensive representation for classification tasks. A traditional solution for dimension reduction in such problems is to concatenate vectors from different views into a new feature space and apply conventional feature selection algorithms such as a CUR factorization straightforwardly on the merged feature set. Another strategy is the separation strategy, which involves performing traditional feature selection on each view separately. However, the concatenation strategy may ignore the specific statistical property of each feature set, and the separation strategy may fail to capture the relations between the views. In general, multiple views of data can provide

complementary information. Hence, it is reasonable to construct a feature selection algorithm that studies multiple views together and exploits relations among them. An RSVD-CUR factorization may serve as an unsupervised feature selection for two-view data, which makes the most of the correlation between the views.

We compare the classification test error rate of the Q-DEIM type RSVD-CUR scheme with that of the Q-DEIM type CUR algorithm. Let the first view/feature set be matrix  $B$  and the second view be matrix  $G$ . We construct the following reduced feature sets and compare their classification performance:

- (i) We generate two reduced feature sets by applying the DEIM-CUR procedure on each view (separation strategy). We label the reduced feature sets CUR-View1 and CUR-View2.
- (ii) We create another two reduced feature sets by performing RSVD-CUR using the two, i.e., RSVD-CUR of  $(B^T G, B^T, G)$ . We label them RSVD-CUR-View1 and RSVD-CUR-View2, which are the RSVD-CUR selected features of views 1 and 2, respectively.
- (iii) The feature set labelled Fused-CUR is a concatenation of the two reduced feature sets from (i), i.e., [CUR-View1, CUR-View2].
- (iv) We also form another feature set labelled Concat-CUR by running the DEIM-CUR scheme on the column concatenation of both views (note that here, the concatenation of the views is done before the dimension reduction is performed).
- (v) Lastly, we concatenate the two reduced feature sets from (ii) to get Fused-RSVD-CUR, i.e., [RSVD-CUR-View1, RSVD-CUR-View2].

For a fair comparison, we compare the results of the single views, i.e., the reduced feature sets from (i) and (ii) in one figure and compare the results of the feature fusion, i.e., (iii), (iv) and (v) in a different plot. The first comparison illustrates how incorporating complementary information from all views in selecting the “best” features of each feature set may help improve their respective classification performance. In the second comparison, our goal is to investigate if using features of all views improves the classification results and also which method yields the best results.

For this experiment, we use two types of real-life data sets to evaluate the effectiveness of our approach. The basic information related to the used multi-view data sets is as follows:

- (1) The handwritten digits data set from the UCI repository, containing features of handwritten numerals (‘0’-‘9’) extracted from a collection of Dutch utility maps. The data set has 2000 digits with 200 instances for each of the ten classes. Three types of feature sets have been extracted: Fourier descriptors, Karhunen-Loève coefficients, and image vectors. The Fourier set consists of 76 two-dimensional shape descriptors. The Karhunen-Loève feature set consists of 64 features. The ‘pixel’ feature set was obtained by dividing the image of  $30 \times 48$  pixels into 240 tiles of  $2 \times 3$  pixels. We combine these three feature sets to form three experiments on multi-view classification. In the first experiment, we take the Fourier coefficients of the character shapes (**fou**) and the Karhunen-Loève coefficients (**kar**) as view-1 and view-2, respectively. The second experiment has the pixel averages in  $2 \times 3$  windows (**pix**) as the first view and the Fourier coefficients of the character shapes (**fou**) as the second view. The final experiment takes the pixel averages in  $2 \times 3$  windows (**pix**) as the first view and the Karhunen-Loève coefficients (**kar**) as the second view.
- (2) The Caltech-101 data set comprises images of objects belonging to 101 classes.

This data set is commonly used to train and test computer vision recognition and classification. We perform the experiment using the Caltech-20 data set, which is a subset of the Caltech-101 data set containing 20 classes<sup>3</sup>. The data set consists of 2386 samples, we chose two representative feature views: the local binary patterns (lbp) feature and the gist feature set of dimensions 928 and 512, respectively.

Table 3 summarizes the basic traits of the various data sets. We normalize all the data sets to have zero center and a standard deviation of one.

TABLE 3  
Summary characteristics of multiview data sets used in the experiments.

Data set	Samples	View 1 ( $B$ )	View 2 ( $G$ )
Digits (fou vs. kar)	2000	76	64
Digits (pix vs. fou)	2000	240	76
Digits (pix vs. kar)	2000	240	64
Caltech-20 (lbp vs. gist)	2386	928	512

In each experiment, we randomly split the normalized data into 75% train and 25% test data. For the randomization of the experiments, we perform 20 cases using different random seeds. Figures 4 and 5 reports the average classification test error rate of the default  $k$ -nearest neighbor ( $k$ -NN) classifier in MATLAB for varying reduced dimensions.

From Figures 4 and 5, we observe that an RSVD-CUR method consistently performs better than a CUR scheme. In particular, from the classification results using single views, the RSVD-CUR significantly improves the worse CUR single view results, as seen in Figure 4. We notice that using information from multiple views indeed reduces the classification test error rate. Furthermore, in Figure 5, we observe that feature fusion from an RSVD-CUR approximation gives the least test error rate compared with the two other approaches involving the CUR scheme, i.e., method (iii) and (iv).

*Experiment 5.4.* Our next experiment illustrates how an RSVD-CUR decomposition may be viewed as a supervised feature selection technique for multi-label classification problems. In contrast to multi-class classification in which instances can only belong to a single class, in multi-label classification problems instances can belong to more than one class at a time. Traditional supervised feature selection techniques are usually for binary/multi-class problems. They may be suitable for multi-label data sets after transforming the data set by using some transformation methods such as label powerset and binary relevance [20].

An RSVD-CUR decomposition provides an alternative way, which does not require transforming the data set. This decomposition exploits some of the basis vectors that maximize the cross-correlation across the feature and output spaces. This may be considered an obvious advantage that the RSVD-CUR has over the CUR factorization since the latter can only be used as an unsupervised feature selection technique. Here we take the feature space as the matrix  $B$  and the response space as the matrix  $G$ . Note that one can reduce the dimension of the feature space to at most the number of class labels (if the number of features is greater than the number of class labels).

Using three benchmark multi-label data sets from the Mulan database<sup>4</sup>, we investigate the performance of the DEIM type RSVD-CUR (which incorporates information

<sup>3</sup>[http://www.vision.caltech.edu/Image\\_Datasets/Caltech101/](http://www.vision.caltech.edu/Image_Datasets/Caltech101/)

<sup>4</sup><http://mulan.sourceforge.net/datasets-mlc.html>

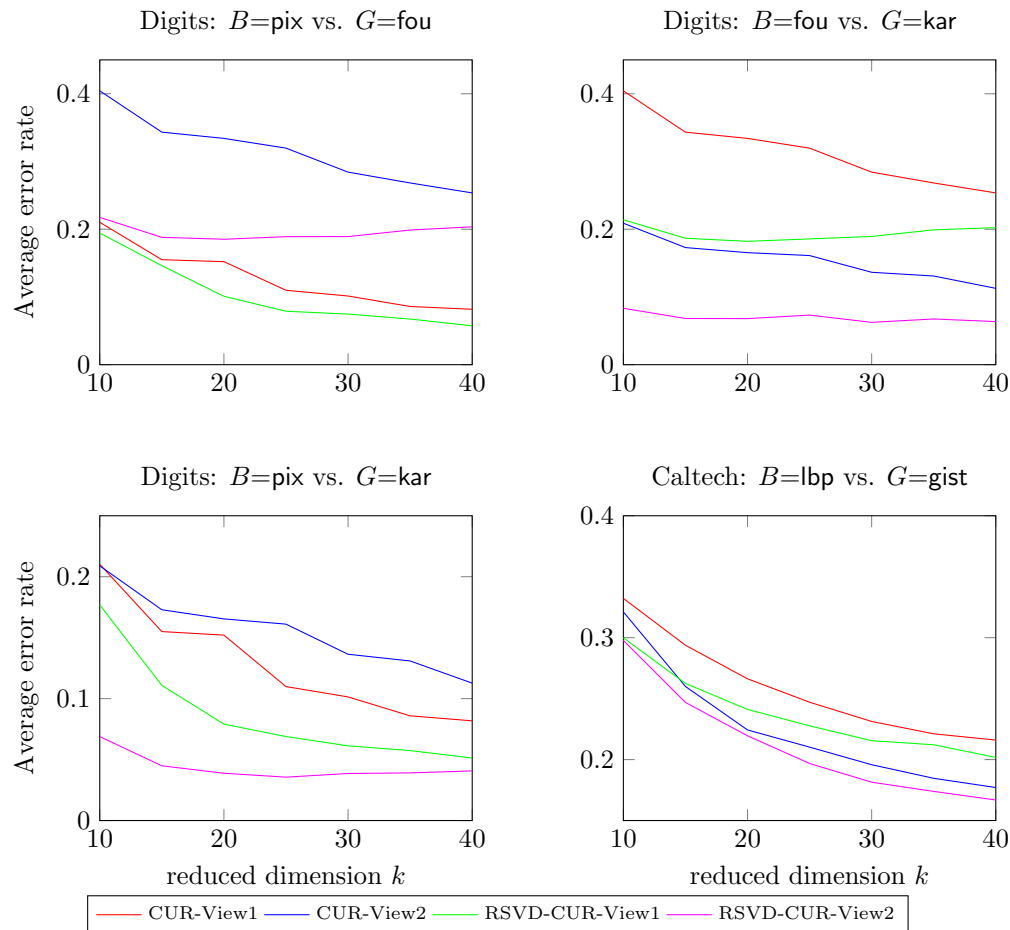


FIG. 4. The average classification test error rate over 20 different random train-test splits of the Fourier descriptors and feature set using CUR and RSVD-CUR as a dimension reduction method for a  $k$ -nearest neighbor classifier in Experiment 5.3. The average classification error as a function of reduced dimensions  $k$ . The  $k$  values of the combined views (second row) are twice that of the single views (first row).

from the output space) as a feature selection technique for multi-label classification problems compared with the DEIM type CUR. The characteristics of the data sets are summarized in Table 4. The data sets come from two domains: biology and text categorization.

- (1) From the biological domain, we have the yeast data set, which contains microarray expression data and phylogenetic profiles. There are 103 descriptive features per gene. A subset of 14 functional classes from the comprehensive yeast genome database<sup>5</sup> is used as the labels. Each gene can be associated with more than one functional class.
- (2) The bibtex and bookmarks data sets are based on the data of the ECML/PKDD 2008 discovery challenge. The former comprises 7,395 *bibtex* entries from the BibSonomy social bookmark and publication sharing system, anno-

<sup>5</sup><https://pubmed.ncbi.nlm.nih.gov/15608217/>

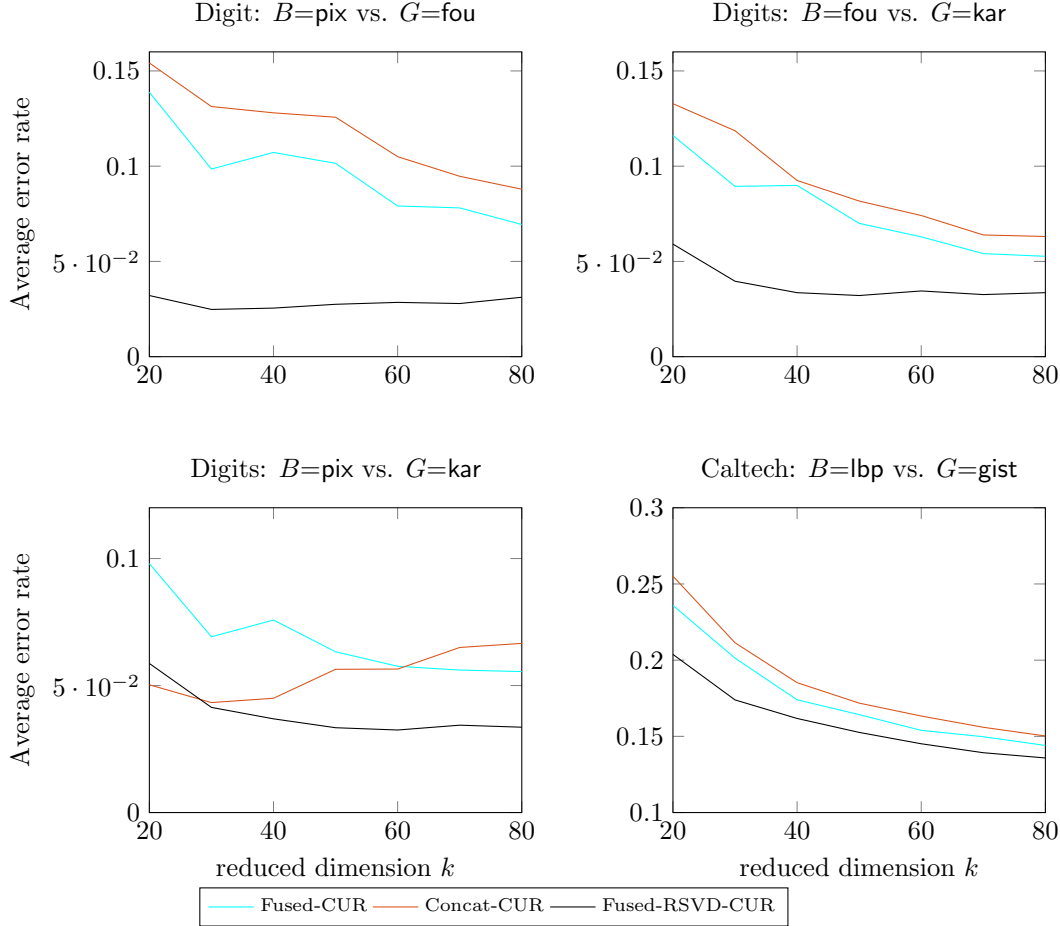


FIG. 5. The average classification test error rate over 20 different random train-test splits of the ‘pixel’ and Karhunen-Loève feature set using CUR and RSVD-CUR as a dimension reduction method for a  $k$ -nearest neighbor classifier in Experiment 5.3. The average classification error as a function of reduced dimensions  $k$ . The  $k$  values of the combined views (second row) are twice that of the single views (first row).

tated with a subset of the tags assigned by Bibsonomy<sup>6</sup> users. Metadata for BibTeX items, such as the title of the paper, the authors, book title, journal volume, publisher, etc., were used to construct features using the boolean bag-of-words model. The bookmarks data set contains metadata for bookmark items, such as the URL of the web page, an URL hash, a description of the web page, etc., and has 87,856 entries.

Using both the original and reduced feature sets, we train two multi-label classifiers, i.e., the classifier chains (CC) developed by Read et al. [24] and the binary relevance (BR) proposed by Godbole and Sarawagi [13], with logistic regression classifier as the baseline. We use the default arguments of the various classifiers as implemented in the sklearn package.

Aside the bookmarks data set, the rest of the data sets are already separated into

<sup>6</sup><https://www.bibsonomy.org/>

training and test sets in the Mulan database. For convenience, we first randomly select 50% of the samples in the `bookmarks` data set and then randomly split that into 80% train set and 20% test set. To assess the performance of the classifiers after the feature selection process, we employ the micro average F1 score (a label-based metric) and the hamming loss (a sample-based metric) [20]. For the F1 score, a higher value indicates good performance. On the other hand, for hamming loss, a lower value implies good performance. We emphasize that the goal here is to evaluate which reduced feature set produces a better classification result (we are not concerned about which classifier is the best).

TABLE 4  
*Basic traits of multi-label data sets used in the experimentation.*

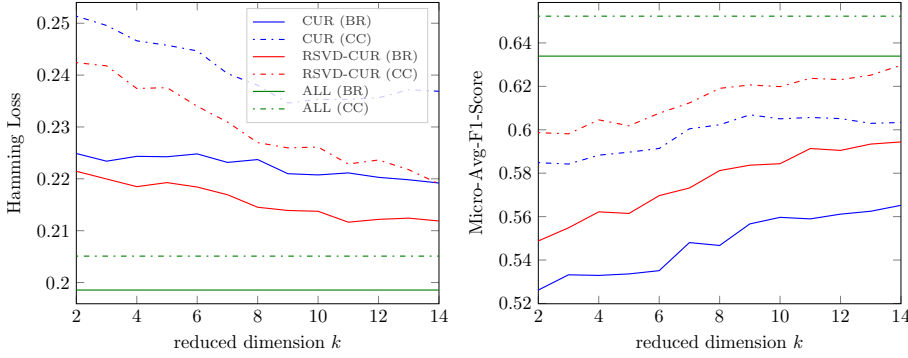
Data set	Domain	Samples	Features ( $B$ )	Class labels ( $G$ )
yeast	biology	2417	103	14
bibtex	text	7395	1836	159
bookmarks	text	87856	2150	208

In Figure 6, we observe that incorporating information from the output space in the process of selecting the features, i.e., the RSVD-CUR method yields better classification results than a CUR method irrespective of the classifier used. For the `bookmarks` data set, we see that the features selected by the RSVD-CUR scheme produce only a slight improvement over those picked by the CUR method for both evaluation metrics. For the other two data sets, the improved results of using the features selected by the RSVD-CUR scheme are very apparent (we include the performance of the classifiers using all the original features as reference only).

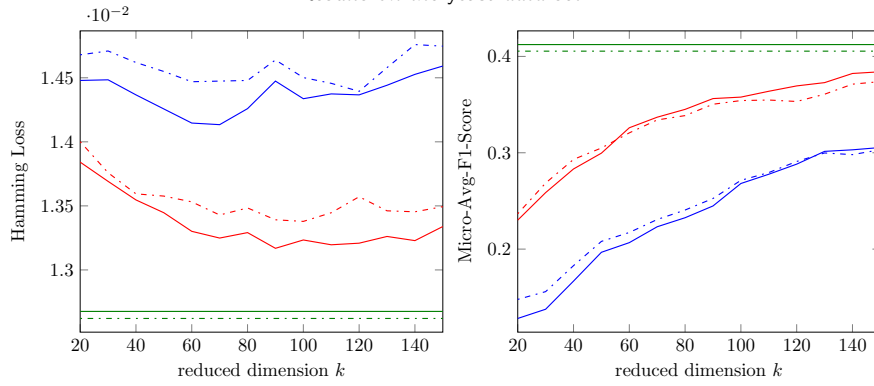
*Experiment 5.5.* In some applications, a user is not only interested in selecting the “best” subset of features, but also in reducing costs that may be associated with those features. For instance, for medical diagnosis, symptoms observed by medical practitioners or patients may be cost-free, but each diagnosis determined by a medical test is associated with its own cost and risk. It is, therefore, crucial to save monetary costs and also relieve the patient of going through risky or unpleasant clinical tests (variables that can be quantified as costly). In the image analysis domain, the computational expense of features usually constitutes the time and space complexities of the feature acquisition processes. Modelers are often interested in reducing this cost by considering only relevant variables, which are also ideally “inexpensive”.

In the presence of correlated noise, we aim to evaluate the CUR, GCUR, and RSVD-CUR methods in selecting relevant features that can improve prediction while keeping feature acquisition costs low. To demonstrate how the RSVD-CUR factorization can be used in this context we employ the Thyroid disease data set from the UCI repository. The problem is to determine whether a patient referred to the clinic is hypothyroid. The three classes in the data set are: normal (not hypothyroid), hyperfunction and subnormal functioning. Because 92% of the patients are not hyperthyroid, a good classifier should have accuracy significantly better than 92%. This 21-dimensional data set has a separate training and testing set. The training set consists of 3772 samples and the testing set consists of 3428 instances. The data set comes with an intrinsic cost associated with 20 input features, which we used to construct a diagonal matrix  $G \in \mathbb{R}^{20 \times 20}$ . We, therefore, dropped the feature that does not have an associated cost. Table 5 show the Thyroids data set attributes. For our purpose, we add a small correlated noise perturbation to the normalized train data set, e.g.,  $\varepsilon = \|A_E - A\|/\|A\| = 0.001$ , where matrix  $A$  represents the original 20-

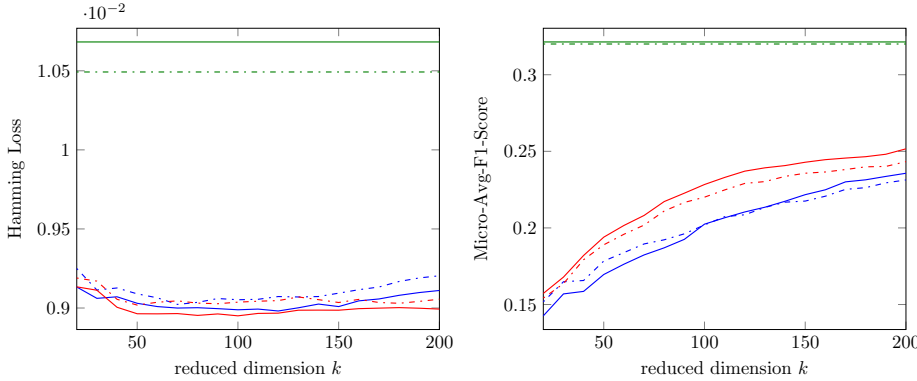




Results on the yeast data set.



Results on the bibtex data set.



Results on the bookmarks data set.

FIG. 6. The hamming loss and micro average F1 measure of each data set using CUR and RSVD-CUR as a feature selection method for classifier chains (CC) and binary relevance (BR) multi-label classifiers in Experiment 5.4. The evaluation metrics (on the vertical axis) as a function of reduced dimensions  $k$  (on the horizontal axis).

dimensional train data set (Note that we only perturb the train data set.). We assume that the lower triangular matrix  $B \in \mathbb{R}^{3772 \times 3772}$  is the Cholesky factor of a symmetric positive definite matrix with first-order autoregressive structure (5.2) (with diagonal entries 1 and the off-diagonal entries related by a multiplicative factor of 0.99). So

TABLE 5  
*Thyroid disease data features and their associated costs.*

Feature	Cost	Feature	Cost
age	1.00	query_hyperthyroid	1.00
sex	1.00	lithium	1.00
on_thyroxine	1.00	goitre	1.00
query_on_thyroxine	1.00	tumor	1.00
on_antithyroid_medication	1.00	hypopituitary	1.00
sick	1.00	psych	1.00
pregnant	1.00	TSH	22.78
thyroid_surgery	1.00	T3	11.41
I131_treatment	1.00	TT4	14.51
query_hypothyroid	1.00	T4U	11.41

the perturbation matrix  $E = B\tilde{E}$ , where  $\tilde{E} \in \mathbb{R}^{3772 \times 20}$  is a random Gaussian matrix.

We compare the cost of features selected and the classification test error rates for each algorithm. The CUR decomposition is used to pick a subset of 10 columns of  $A_E$  without considering the noise filter  $B$  and cost matrix  $G$ . The GCUR of  $(A_E, G)$  selects a subset of 10 columns of  $A_E$  relative to  $G$  (here also, we do not take the noise into account). The RSVD-CUR of  $(A_E, B, G)$  chooses 10 columns of  $A_E$  by incorporating all available prior information. For the randomization of the experiment, we perform 10 cases using different random seeds. Table 6 reports the average classification test error rate and the average cost of select of the default  $k$ -nearest neighbour ( $k$ -NN) classifier in MATLAB. We observe in Table 6 that methods

TABLE 6  
*Average classification test error rate and total cost of selected variables using data set in Experiment 5.5. The  $k$ -NN model is trained using the perturbed train data set.*

Method/Criteria	Error rate		Cost
	$\varepsilon = 10^{-4}$	$\varepsilon = 10^{-3}$	
RSVD-CUR	0.07	0.07	10
GCUR	0.09	0.26	10
CUR	0.11	0.11	23.51
All features	0.07	0.07	76.11

that incorporate the cost information in the selection of the variables (i.e., GCUR and RSVD-CUR) yield lower total costs of features. The features selected by the RSVD-CUR produce the least classification error rate, which may be because the RSVD-CUR includes the noise structure in the feature selection process. Where  $\varepsilon = 0.0001$ , we have an improvement in the classification average error rate of the RSVD-CUR to be about 28% and 57% over the GCUR and CUR, respectively. We also observe that, the error rates of the RSVD-CUR and CUR factorizations are not very sensitive to the level perturbation as opposed to those of the GCUR decomposition (i.e., the error rate of the features selected by the GCUR increases drastically from 0.09 to 0.26 when the noise level increases from 0.0001 to 0.001). Additionally, the error rate of using the whole feature set (20-dimensional) is comparable to that of the RSVD-CUR, which is 10-dimensional and with a lower cost of features. Where  $\varepsilon = 0.001$  both the RSVD-CUR and the GCUR decompositions select the variable “pregnant” (which is one of the least costly features) as the most important. On the other, the CUR factorization picks the “TT4” attribute (the second most costly variable) as the most important, which is why its cost of features is the highest compared to the GCUR and RSVD-CUR approaches.

**General Gauss-Markov model with constraints.** We briefly describe another possible application of the RSVD-CUR factorization here.

The RSVD-CUR decomposition may be used as a subset selection procedure in the general Gauss-Markov linear models with constraints problem (1.2). “This problem formulation admits ill-conditioned or singular  $B \in \mathbb{R}^{m \times \ell}$  and  $G \in \mathbb{R}^{d \times n}$  (usually with  $d \leq n$ ) matrices” [8]. The matrix  $B$  may be considered as a noise filter and  $G$  may represent prior information about the unknown components of  $\mathbf{x}$  or may reflect the fact that certain components of  $\mathbf{x}$  are more important or less costly than others [8]. Minimizing  $\|\mathbf{y}\|^2 + \|\mathbf{f}\|^2$  reflects that the goal is to explain as much in terms of the columns of  $A$  (i.e.,  $\min \mathbf{y}^T \mathbf{y}$ ), taking into consideration the prior information on the structure of the noise as well as the preference of the modeler to use more of one predictor than others in explaining the phenomenon [8]. It is easy to see that the problem has a solution if the linear system

$$\begin{bmatrix} A & B \\ G & 0 \end{bmatrix} \begin{bmatrix} \mathbf{x} \\ \mathbf{y} \end{bmatrix} = \begin{bmatrix} \mathbf{b} \\ \mathbf{f} \end{bmatrix}$$

is consistent.

In many applications, it is desirable to reduce the number of variables that are to be considered or measured in the future. As a result, it would be appropriate to use a variable subset selection method that incorporates all available prior information (i.e.,  $B$  and  $G$ ). Since this problem (1.2) involves three matrices, the RSVD-CUR is a suitable procedure for variable subset selection. One may argue that a CUR decomposition of  $B^{-1}AG^{-1}$  may be used if  $B$  and  $G$  are nonsingular. However, since the above problem admits an ill-conditioned or rank-deficient  $B$ , such a formulation may not always be valid. Supposed we want to select  $k$  columns of each matrix the above linear system reduces to

$$\begin{bmatrix} A_k & B_k \\ G_k & 0 \end{bmatrix} \begin{bmatrix} \mathbf{x}_k \\ \mathbf{y}_k \end{bmatrix} = \begin{bmatrix} \mathbf{b} \\ \mathbf{f} \end{bmatrix},$$

where  $A_k = A(:, \mathbf{p})$ ,  $B_k = (:, \mathbf{p}_B)$ , and  $G_k = G(:, \mathbf{p})$ . The index vectors  $\mathbf{p}$  and  $\mathbf{p}_B$  are obtained by applying Algorithm 4.3 to  $(A, B, G)$ .

*Example 5.6.* The following examples are adapted from [7]. We give results for three problems with  $m = 1000$ ,  $n = 100$ ,  $\ell = 50$ , and  $d = 10$ . We denote by `randn` a matrix or vector from the standard normal distribution and by `randsvd( $\kappa$ )` a random matrix with spectral norm condition number  $\kappa$  and geometrically distributed singular values, generated by the routine `randsvd` in the Matlab Test Matrices gallery. We consider problems where either one of the matrices is ill-conditioned.

For all problems, we take  $\mathbf{b} = \text{randn}$  and  $\mathbf{f} = \text{randn}$ . Table 7 reports the average residuals of 100 test cases for each problem using the original and reduced system. We observe with an RSVD selection, the fit of the reduced system in the constrained generalized least squares problem is comparable to that of the full system.

**6. Conclusions.** We have proposed a new low-rank matrix decomposition, an RSVD-CUR factorization with pseudocode in Algorithm 4.3. This factorization is an extension of a CUR decomposition to matrix triplets. Here, we mainly use the DEIM index selection procedure to construct the  $C$  and  $R$  factors of this factorization. Note that other than this index selection scheme, one may use alternative selection methods such as column-pivoted QR decomposition [9] or maximum volume algorithm [15] on the matrices from the RSVD. We have discussed the connection between this DEIM type RSVD-CUR of  $(A, B, G)$  and the DEIM type CUR of  $B^{-1}AG^{-1}$  for nonsingular

TABLE 7

Average residuals of the original and reduced system for varying  $k$  values in parenthesis using the various problems of *Example 5.6*.

Problem \ $k$			10	20	30	Full
$A$	$B$	$G$				
randsvd(10)	randsvd( $10^4$ )	randn	31.5	31.2	30.8	29.4
randsvd( $10^6$ )	randsvd(10)	randn	31.5	31.2	30.8	29.4
randsvd( $10^4$ )	randsvd( $10^4$ )	randsvd(10)	31.4	31.1	30.8	29.3
randn	randn	randn	31.4	31.1	30.8	29.3

$B$  and  $G$ . In a particular case where  $B = I$  and  $G = I$ , the RSVD-CUR decomposition of  $A$  coincides with a CUR decomposition of  $A$ , in that the factors  $C$  and  $R$  of  $A$  are the same for both methods, i.e., the first line of (4.1) is equal to (1.1). We have also pointed out the connection between the DEIM type RSVD-CUR of  $(A, B, G)$  and the DEIM type GCUR of  $(A, G)$  when  $B = I$ , and similarly for the transpose of  $(A, B)$  when  $G = I$ .

An RSVD-CUR factorization may be suitable for feature fusion and applications where one is interested in selecting a subset of features in one data set relative to two other data sets. For subset selection in a multi-view classification problem where two feature sets are available, the new method may yield better classification accuracy than the standard CUR decomposition as shown in the numerical experiments. The proposed method may also be used as a supervised feature selection technique in multi-label classification problems. Additionally, an RSVD-CUR approximation may be useful in data perturbation problems of the form  $A_E = A + BFG$ , where  $BFG$  is a correlated noise matrix and  $B, G$  are matrices of a known structure. An RSVD-CUR decomposition can provide more accurate approximation results compared to a CUR factorization when reconstructing a low-rank matrix from a data matrix perturbed with nonwhite noise. As shown in section 5 we do not necessarily need to know the exact noise covariance matrices; the RSVD and RSVD-CUR may still deliver good approximation results given inexact Cholesky factors  $B$  and  $G$  of the noise covariance matrices. Furthermore, we also demonstrate how one may use the RSVD-CUR factorization as a subset selection technique in generalized Gauss-Markov problems with constraints.

**Acknowledgment.** The authors thank Ian Zwaan for several helpful discussions on algorithms for computing a restricted singular value decomposition. The authors would also like to express special thanks to the referees and editor, whose helpful expert suggestions led to significant improvements in the content and presentation of the paper.

## REFERENCES

- [1] R. ARORA AND K. LIVESCU, *Multi-view CCA-based acoustic features for phonetic recognition across speakers and domains*, in Proc. Int. Conf. Acoust. Speech Signal Proces., 2013, pp. 7135–7139.
- [2] M. BARRAULT, Y. MADAY, N. C. NGUYEN, AND A. T. PATERA, *An ‘empirical interpolation’ method: Application to efficient reduced-basis discretization of partial differential equations*, Comptes Rendus Math., 339 (2004), pp. 667–672.
- [3] A. BECK, *The matrix-restricted total least-squares problem*, Signal Process., 87 (2007), pp. 2303–2312.
- [4] S. CHATURANTABUT AND D. C. SORENSEN, *Nonlinear model reduction via discrete empirical interpolation*, SIAM J. Sci. Comput., 32 (2010), pp. 2737–2764.
- [5] X. CHEN, L. HAN, AND J. CARBONELL, *Structured sparse canonical correlation analysis*, in Proc. Artif. Intell. Statistics Conf., 2012, pp. 199–207.

- [6] D. CHU, L. DE LATHAUWER, AND B. DE MOOR, *On the computation of the restricted singular value decomposition via the cosine-sine decomposition*, SIAM J. Matrix Anal. Appl., 22 (2000), pp. 580–601.
- [7] A. J. COX AND N. J. HIGHAM, *Row-wise backward stable elimination methods for the equality constrained least squares problem*, SIAM J. Matrix Anal. Appl., 21 (1999), pp. 313–326.
- [8] B. L. DE MOOR AND G. H. GOLUB, *The restricted singular value decomposition: properties and applications*, SIAM J. Matrix Anal. Appl., 12 (1991), pp. 401–425.
- [9] Z. DRMAC AND S. GUGERCIN, *A new selection operator for the discrete empirical interpolation method—Improved a priori error bound and extensions*, SIAM J. Sci. Comput., 38 (2016), pp. A631–A648.
- [10] Z. DRMAC AND A. K. SAIBABA, *The discrete empirical interpolation method: Canonical structure and formulation in weighted inner product spaces*, SIAM J. Matrix Anal. Appl., 39 (2018), pp. 1152–1180.
- [11] O. FRIMAN, M. BORGA, P. LUNDBERG, AND H. KNUTSSON, *Adaptive analysis of fMRI data*, NeuroImage, 19 (2003), pp. 837–845.
- [12] P. Y. GIDISU AND M. E. HOCHSTENBACH, *A generalized CUR decomposition for matrix pairs*, SIAM J. Math. Data Science, 4 (2022), pp. 386–409.
- [13] S. GODBOLE AND S. SARAWAGI, *Discriminative methods for multi-labeled classification*, in Pacific-Asia Conference on Knowledge Discovery and Data Mining, Springer, Berlin, Heidelberg, 2004, pp. 22–30.
- [14] G. H. GOLUB AND H. ZHA, *The canonical correlations of matrix pairs and their numerical computation*, in Linear Algebra for Signal Processing, Springer, 1995, pp. 27–49.
- [15] S. A. GOREINOV, I. V. OSELEDETS, D. V. SAVOSTYANOV, E. E. TYRTYSHNIKOV, AND N. L. ZAMARASHKIN, *How to find a good submatrix*, in Matrix Methods: Theory, Algorithms And Applications, World Scientific, Singapore, 2010, pp. 247–256.
- [16] S. A. GOREINOV, N. L. ZAMARASHKIN, AND E. E. TYRTYSHNIKOV, *Pseudo-skeleton approximations by matrices of maximal volume*, Math. Notes, 62 (1997), pp. 515–519.
- [17] N. HALKO, P. G. MARTINSSON, AND J. A. TROPP, *Finding structure with randomness: Probabilistic algorithms for constructing approximate matrix decompositions*, SIAM Review, 53 (2011), pp. 217–288.
- [18] P. C. HANSEN, *Rank-Deficient and Discrete Ill-Posed Problems: Numerical Aspects of Linear Inversion*, SIAM, Philadelphia, 1998.
- [19] W. K. HÄRDLE AND L. SIMAR, *Applied Multivariate Statistical Analysis*, Springer, Berlin, Heidelberg, 4th ed., 2015.
- [20] F. HERRERA, F. CHARTE, A. J. RIVERA, AND M. J. DEL JESUS, *Multilabel Classification: Problem Analysis, Metrics and Techniques*, Springer, Switzerland, 2016.
- [21] R. A. HORN AND C. R. JOHNSON, *Matrix Analysis*, Cambridge University Press, 2nd ed., 2012.
- [22] M. W. MAHONEY AND P. DRINEAS, *CUR matrix decompositions for improved data analysis*, Proc. Natl. Acad. Sci. USA, 106 (2009), pp. 697–702.
- [23] N. RASIWASIA, J. C. PEREIRA, E. COVIELLO, G. DOYLE, G. R. LANCKRIET, R. LEVY, AND N. VASCONCELOS, *A new approach to cross-modal multimedia retrieval*, in Proc. Int. Conf. Multimedia, ACM, 2010, pp. 251–260.
- [24] J. READ, B. PFAHRINGER, G. HOLMES, AND E. FRANK, *Classifier chains for multi-label classification*, Mach. Learn., 85 (2011), pp. 333–359.
- [25] D. C. SORENSEN AND M. EMBREE, *A DEIM induced CUR factorization*, SIAM J. Sci. Comput., 33 (2016), pp. A1454–A1482.
- [26] G. W. STEWART, *Four algorithms for the efficient computation of truncated pivoted QR approximations to a sparse matrix*, Numer. Math., 83 (1998), pp. 313–323.
- [27] D. B. SZYLD, *The many proofs of an identity on the norm of oblique projections*, Numer. Algorithms, 42 (2006), pp. 309–323.
- [28] C. F. VAN LOAN, *Generalizing the singular value decomposition*, SIAM J. Numer. Anal., 13 (1976), pp. 76–83.
- [29] S. VORONIN AND P. G. MARTINSSON, *Efficient algorithms for CUR and interpolative matrix decompositions*, Adv. Comput. Math, 43 (2017), pp. 495–516.
- [30] R. WICKLIN, *Simulating Data with SAS*, SAS Institute, 2013.
- [31] C. XU, D. TAO, AND C. XU, *A survey on multi-view learning*, 2013, <https://arxiv.org/abs/1304.5634>.
- [32] H. ZHA, *The restricted singular value decomposition of matrix triplets*, SIAM J. Matrix Anal. Appl., 12 (1991), pp. 172–194.
- [33] I. N. ZWAAN, *Towards a more robust algorithm for computing the restricted singular value decomposition*, 2020, <https://arxiv.org/abs/2002.04828>.